The Possible Consequences of Rapidly Depressurizing a Fluid

by

Miral Eonhah Kim-E

B.S., California Institute of Technology
(1978)

SUBMITTED IN PARTIAL FULFILLMENT
OF THE REQUIREMENTS FOR THE
DEGREE OF

MASTER OF SCIENCE IN
CHEMICAL ENGINEERING

at the

MASSACHUSETTS INSTITUTE OF TECHNOLOGY

January 1981

Signature of Author_____

Department of Chemical Engineering
January 16, 1981

Certified by_____

Robert C. Reid
Thesis Supervisor

Accepted by_____

Glenn C. Williams
Chairman, Departmental Graduate Committee

The Possible Consequences of Rapidly Depressurizing a Fluid

by

Miral Eonhah Kim-E

Submitted to the Department of Chemical Engineering on January 16, 1981 in partial fulfillment of the requirements for the Degree of Master of Science in Chemical Engineering

ABSTRACT

The rapid depressurization of liquids, such as that which might occur in an LPG tank car accident, has been known to lead to violent explosions. An experiment was devised to test a possible mechanism for these depressurization explosions (also known as BLEVE's) which involves that fluid's limit of thermodynamic stability. A seven-liter, cylindrical container, containing liquid or supercritical carbon dioxide, was depressurized using a 1.5-inch burst disc system. Results were inconclusive due to rapid vapor formation and the inability to measure the temperatures of the fluid and the walls. However, a comparison of characteristic times for the processes that occur during depressurization indicate that the proposed mechanism is a plausible model for depressurization explosions.

Thesis Supervisor : Dr. Robert C. Reid

Title : Professor of Chemical Engineering

to my family:

Mulka

Grace

and

Rhoda

ACKNOWLEDGEMENTS

I am grateful to Mr. Donald Wetherilt and his associates at Westreco for supplying the liquid-holding container so vital to this study.

And to my friends in the LNG lab, thanks for good advice, endless encouragement, and many fun-filled hours whenever we were together. I wish you all success, happiness, and lasting friendship in the years to come.

Finally, I only wish that I were eloquent enough to truly express how fortunate I feel to have had the opportunity to work with Bob Reid. Thanks, Bob, for teaching clearly, understanding often, and caring so much.

Table of Contents

List of Figures

List of Figures, cont'd.

INTRODUCTION

Evidence is rapidly accumulating which indicates that if a vessel, containing a fluid at high pressures and at temperatures near or exceeding its critical temperature, experiences an extremely rapid depressurization, a detonation may occur. LPG (liquefied petroleum gas) tank cars which have been subject to an external fire, have, on occasion, undergone rapid tank failure - with concomitant depressurization - and violently exploded. These blasts have become known as "Boiling Liquid Expanding Vapor Explosions", or BLEVE's, since such an explosion is probably linked to the fact that a large mass of liquid is expanding in a boiling process in a very short period of time. Since it is relatively common for engineers to be in situations that necessitate the containment of such fluids (e.g., storage tanks, reactors), this concept of a "depressurization explosion" phenomenon encourages further study.

Rapid depressurization of these vessels is usually the result of an accident that permits nearly instantaneous venting of the contents. Of course, most accidents occur quite unexpectedly, hence, very little is known about the sequence of events and the conditions of the fluid prior to the mishap. In order to gain and understanding of the mechanism of LPG tank car BLEVE's, the United States Department of Transportation performed a study (Anderson et al. 1974) in which a rail tank car, filled with LPG, was engulfed in a kerosene fire; the temperature and pressure of the car's contents were monitored throughout the experiment.

Due to the intense heat, a localized stress failure in the non-wetted wall is believed to have occurred. A subsequent explosion/shock wave fragmented the tank car. Just prior to the explosion the liquid temperature

was measured at 342 K (0.93 T_c) and the pressure, 22 bar.

With LPG (i.e., propane), one might expect that the explosion is due to a rapid combustion process of some sort, but the fact that similar explosions involving carbon dioxide (Leiber 1979, Copeland 1976) have been reported seems to rule out the possibility of chemical reactions being central to the cause of depressurization explosions. In addition, the phenomenon is not restricted to large scale accidents; fire extinguisher failures (Burghard and Wangler 1979), due to stress corrosion cracking of the wall, have been reported to result in considerable damage.

As yet, there is no definitive explanation for the creation of the shock wave that might accompany a depressurization accident. Ogiso et al. (1972) attributed such an explosion to rapid boiling of the superheated liquid that results from the sudden depressurization: the so-called "water hammer effect". Reid (1979) has taken this one step further by suggesting that the depressurization follows a thermodynamic path such that the liquid may reach its superheat-limit locus of states (also known as the "spinoidal curve") and that no true explosion will result unless this limit is reached. These mechanisms can be illustrated on a pressure-temperature diagram for a pure substance (Figure 1).

A pure fluid under high pressure in a closed vessel will exist in a saturated or supercritical state. If the depressurization is rapid, there may not be enough time for boiling to be initiated on the tank walls, so the thermodynamic path followed by the fluid will be isentropic and will enter into the superheated liquid regime (between the saturation and spinoidal curves). If the depressurization is slow, there will be time for boiling to occur, so the liquid will never become appreciably superheated.

So, for a slow depressurization, both models predict no explosion since a superheated liquid is never obtained. But for a very rapid

depressurization, Ogiso's model indicates that all paths that enter the superheated liquid region will result in explosion and Reid's model indicates that only those paths that can reach the spinoidal curve will produce explosions. For example, a fluid initially at state A or A_s will reach the spinoidal curve at state B upon rapid depressurization and the liquid will vapor explode. But if the fluid is initially at C or C_s, a depressurization will lead to a superheated liquid at one bar (atmospheric pressure); rapid boiling will ensue, but no explosion. So the boundary between initial states that lead to depressurization explosions and those that do not is the locus of states that lie on the isentropic curve that passes through the liquid spinoidal curve at one bar.

The hypothesis that superheated liquids may play a role in regards to depressurization explosions is not a completely unfounded conjecture. Superheated liquids have been proved to cause vapor explosions in situations quite different than the one presently being addressed: hot liquid - cold liquid contact. Usually as the result of an accident, a very hot liquid comes into intimate contact with a cold liquid, e.g., molten aluminum spilled into water. If the hot liquid is sufficiently hot to superheat the cooler liquid to the spontaneous nucleation temperature, the superheated liquid will vapor explode.

The main thrust of this work has been to determine experimentally the role of superheated liquids in depressurization explosions. Of course, the ultimate goal in all studies of these types of phenomenon is to develop criteria by which an accurate assessment of the hazards involved can be made.

SUPERHEATED LIQUIDS AND NUCLEATION

As mentioned previously, a superheated liquid lies in the region between the saturation and spinoidal curves. This is illustrated in Figure 2, which represents a typical pressure-volume diagram, with lines of constant temperature, for a pure fluid. At a given pressure, a superheated liquid exists at a temperature that is higher than one would expect based on the more common observance of saturated liquids, hence the term "superheated". These are thermodynamically metastable states, since small perturbations to such systems will drive them to more stable states. (There is an analogous situation on the other side of the P-V dome: subcooled vapors. Since subcooled vapors will tend to condense to form liquid phases, rather than expand, it is unlikely that these states could be involved in depressurization explosions.) The spinoidal curve represents the limit to the degree of superheat a liquid can obtain and is predictable from thermodynamic or kinetic considerations. Note that the critical point lies on both the saturation and spinoidal curves.

In order to understand why superheated liquids can exist, consider a small cluster of liquid molecules (on the order of ten molecules) in a moderately superheated liquid. If this cluster forms a vapor bubble without the benefit of the presence of other phases (solid, gaseous, or another immiscible liquid phase), then "homogeneous nucleation" is said to have occurred. The net result of bubble formation is to increase the availability of the composite system of liquid and the bubble, and the bubble will tend to collapse back into its original (and lower energy) liquid cluster configuration.

Due to curvature effects, the pressure inside the bubble is greater

than the pressure of the surrounding liquid. However, if we could continue to add molecules to such a bubble, the bubble's pressure would continually decrease as the bubble grows due to the decreasing importance of curvature. Eventually, the availability of the composite system will reach a maximum at some "critical" bubble volume. At this point, the chemical potential of the gas and liquid phases are equal, and any further increase in the bubble size will cause the availability of the system to decrease, since the bubble pressure will continue to fall. This, of course, will cause the bubble to grow spontaneously until all the liquid disappears or both phases reach corresponding saturated states.

The availability necessary to create a critical-sized bubble is an energy barrier to nucleation. In a moderately superheated liquid, statistical fluctuations in the liquid molecules' energy will permit some fraction of the liquid to pass over this barrier and form a vapor phase. If the degree of superheat increases, this fraction will increase, since the average energy of the molecules will also be increased.

However, the presence of a solid surface can change the mechanism of nucleation dramatically. Microscopic cavities on the surface, attributable to the solid's roughness, will sustain vapor bubbles smaller than the critical size. Any superheated liquid that contacts this surface will vaporize into these trapped bubbles until they are large enough to detach, which allows the site to start this "heterogeneous nucleation" process again. This mechanism severely limits the degree of superheat the liquid will achieve, since it offers the liquid an opportunity to be in a more thermodynamically stable configuration. Of course, this effect can be offset by making the solid surface very smooth, as in clean glass.

In the absence of heterogeneous nucleation sites, a liquid can theore-

tically be superheated to its maximum value. Upon reaching its spinoidal curve, the liquid will experience spontaneous homogeneous nucleation. This phenomenon is observed experimentally in bubble columns: small drops of the test liquid are injected into the bottom of the column which contains a denser fluid with an externally applied vertical temperature gradient. As the drop rises into the hotter fluid, it is eventually heated to its superheat limit temperature and a vapor bubble suddenly appears, accompanied by a sharp pop.

THERMODYNAMIC CONSIDERATIONS

The derivation of the spinoidal curve from thermodynamic considerations lies in the criterion, first developed by Gibbs in the late 1870's, that an isolated system in a stable equilibrium state will seek to maximize its total entropy. Using Legendre transform theory (Beegle et al. 1974), this can be stated as:

$$y^{(n)}_{(n+1)(n+1)} > 0 \quad \text{for a stable system} \qquad (1)$$

$$y^{(n)}_{(n+1)(n+1)} = 0 \quad \text{for the limit of stability} \qquad (2)$$

where n = number of components in the system

$y^{(n)}$ = n-th Legendre transform of a base representation of the system's energy, $y^{(0)}$

$y^{(n)}_{(n+1)(n+1)}$ = the second order partial derivative of $y^{(n)}$ with respect to the $n+1$ variable

For a pure material, n=1. If we take $y^{(0)}$ as the internal energy, $\underline{U}(\underline{S},\underline{V},N)$, then $y^{(1)}$ is the Helmholtz energy, $\underline{A}(T,\underline{V},N)$. For this choice of basis function and variable order, (1) and (2) become:

$$y^{(1)}_{22} = \left(\frac{\partial^2 \underline{A}}{\partial \underline{V}^2}\right)_{T,N} = -\left(\frac{\partial P}{\partial \underline{V}}\right)_{T,N} > 0 \quad \text{for a stable system} \qquad (3)$$

$$\left(\frac{\partial P}{\partial \underline{V}}\right)_{T,N} = 0 \quad \text{for the limit of stability} \qquad (4)$$

The use of (4) requires an accurate equation of state. The Peng-Robinson equation of state (Peng and Robinson 1976) is appropriate for most

applications; it gives fairly accurate predictions of liquid, as well as vapor, volumes and has only two adjustable parameters. It is given by:

$$P = \frac{R\,T}{V-b} - \frac{a(T)}{V(V+b) + b(V-b)}$$

Details of the Peng-Robinson equation of state are given in Appendix I.

The spinoidal curve for a pure fluid can be readily obtained using (4) and solving the resulting quartic equation for volume:

$$V^4 + (4b-\frac{2a}{RT})V^3 + 2b(b+\frac{a}{RT})V^2 + 2b^2(\frac{a}{RT}-2b)V + b^4 - \frac{2ab^3}{RT} = 0 \qquad (5)$$

For a temperature below the critical, (5) will yield four real roots. One will be less than the saturated liquid volume and another will be greater than the saturated vapor volume; these are disregarded. The two remaining roots lie between the liquid and vapor saturation curves; the smallest root corresponds to the liquid spinoidal curve and the largest to the vapor spinoidal curve.

It is also convenient to use the Peng-Robinson equation of state to determine isentropic depressurization paths with departure functions (see Appendix I) and a computer program (Appendix II). Results for propane and carbon dioxide are given in Figures 3 and 4, respectively.

For multicomponent systems, (2) is still the criterion for finding the stability limit. However, in order to interpret this in terms of more readily obtainable functions, the second order partial derivative in (2) can be related to a determinant of second order partial derivatives (Beegle et al. 1974). For example, the stability limit for a binary mixture of fluids "A" and "B" for $y^{(0)} = \underline{U}(\underline{S},\underline{V},N_A,N_B)$ is given by:

$$\begin{vmatrix} A_{VV} & A_{VA} \\ A_{AV} & A_{AA} \end{vmatrix} = 0$$

where $$A_{VV} = \left(\frac{\partial^2 \underline{A}}{\partial \underline{V}^2}\right)_{T,N_A,N_B} = -\left(\frac{\partial P}{\partial \underline{V}}\right)_{T,N_A,N_B}$$

$$A_{VA} = A_{AV} = \frac{\partial^2 \underline{A}}{\partial \underline{V} \partial N_A} = -\left(\frac{\partial P}{\partial N_A}\right)_{T,\underline{V},N_B}$$

$$A_{AA} = \left(\frac{\partial^2 \underline{A}}{\partial N_A^2}\right)_{T,\underline{V},N_B}$$

The Peng-Robinson equation of state, and its departure functions, can be used for the analysis of multicomponent systems, the only difference being the composition dependence of the parameters a(T) and b. Details are also given in Appendix I.

KINETIC CONSIDERATIONS

To determine the spinoidal curve from kinetic considerations, one must estimate J, the rate at which bubbles are produced in a given volume of liquid, in terms of physical and/or thermodynamic properties of the liquid. This kinetic theory of nucleation, attributed primarily to Volmer and Doring in the late 1930's, considers a steady state growth process, at constant temperature and external pressure, in which a bubble containing n molecules receives just one single molecule from the liquid phase to produce a bubble with n+1 molecules, and vice versa for bubble collapse. When a bubble becomes macroscopic, it is removed from the system and replaced with the same number of liquid molecules. Quantitatively, it will be assumed that a bubble is macroscopic in nature when it contains n_s molecules, where $n_s >> 1$. So, we have a system in which there is a steady flow of one bubble through all sizes up to n_s, which makes J independent of time and bubble size. This allows J to be expressed as (Moore 1959):

$$J = Z(n)\ S(n)\ W_L(n) - Z(n+1)\ S(n)\ W_V(n+1)$$

where $Z(n)$ = the number of bubbles per unit volume of liquid that contain n molecules

$S(n)$ = the surface area available for mass transfer in a bubble of n molecules

$W_L(n), W_V(n)$ = the probabilistic rate at which a single liquid/vapor molecule will vaporize/condense into a bubble of n molecules per unit area per unit time

The solution to this difference equation is given by:

$$J = Z(n_0)\left[\sum_{n=n_0}^{n_s-1} \frac{1}{W_L(n)S(n)\prod_{i=n_0+1}^{n}\frac{W_L(i-1)}{W_v(i)}}\right]^{-1}$$

where n_0 is the number of molecules in a reference bubble.

From classical statistical mechanics, the probability that a particle will leave the liquid (vapor) is inversely proportional to the liquid's (vapor's) partition function per particle, q_L (q_v). Therefore,

$$\frac{W_L(i-1)}{W_v(i)} = \frac{q_v(i)}{q_L} \tag{6}$$

Note that q_L is not a function of bubble size since the liquid phase is assumed to be an infinite medium.

In addition, the q's can be related to the chemical potential, μ, by (Davidson 1962):

$$\mu = \left(\frac{\partial A}{\partial N}\right)_{T,V} = -kT \ln q \tag{7}$$

where k is Boltzmann's constant, T is temperature. These results give:

$$\sum_{i=n_0+1}^{n}\frac{W_L(i-1)}{W_v(i)} = \exp\sum_{i=n_0+1}^{n}\frac{\mu_L - \mu_v(i)}{kT}$$

Takagi (1953) has shown that the above sum of chemical potentials is related to the Helmholtz energy required to form a bubble containing n molecules, ΔA_n, by :

$$\Delta A_{n_0} - \Delta A_n = \sum_{i=n_0+1}^{n}\{\mu_L - \mu_V(i)\}$$

In effect, ΔA_n is the minimum amount of work needed to create a bubble of n molecules since the model we are dealing with inherently assumes a thermal equilibrium between vapor and liquid phases.

If the reference bubble is chosen to be one containing just a single molecule ($n_0 = 1$), then the reference state is simply the liquid itself. This makes ΔA_{n_0} vanish and Z_{n_0} is the molecular density of the liquid, ρ_L; the expression for J then becomes:

$$J = \rho_L \left[\sum_{n=n_0}^{n_s-1} \frac{\exp \{ \Delta A_n/kT \}}{W_L(n)S(n)} \right]^{-1} \qquad (8)$$

The only important contributions to the sum in (8) come from the critical-sized bubble. As mentioned previously, $\mu_L=\mu_v$ at this point, so (6) and (7) imply that $W_v(n_c)=W_L(n_c)$. If we postulate that W_v is identically equal to the frequency with which a vapor molecule will collide with a unit area of bubble-liquid interface, the kinetic theory of gases gives:

$$W_v = \frac{P_v}{Z(2\pi mkT)^{1/2}}$$

where P_v = the pressure within the bubble

Z = the compressibility factor

m = mass of a molecule

ΔA_{n_c} is related to the radius of the spherical critical bubble, r_c, and to surface tension, σ, by:

$$\Delta A_{n_c} = \frac{4}{3} \pi r_c^2 \sigma$$

And r_c can, in turn, be related to pressures within, and external to, the bubble and to σ by (Modell and Reid 1974):

$$r_c = \frac{2\sigma}{(P_v - P_L)}$$

where P_L is the pressure of the liquid phase. With these expressions, J can be expressed in terms of the fluid's physical properties (Blander and Katz 1975) :

$$J = 3.73 \times 10^{35} \left[\frac{d^2\sigma}{M^3 B}\right]^{1/2} \exp\left[\frac{-1.182\times10^5\ \sigma^3}{T(P_v-P_L)^2}\right] \quad (9)$$

where B = 2/3, except for cavitation (B=1)

d = liquid density, g cm^{-3}

M = molecular weight, g $mole^{-1}$

and units for the other quantities are J($cm^{-3}s^{-1}$), σ(erg cm^{-2}), T(K), P_L(atm), and P_v(atm).

Because σ decreases and P_v increases with temperature, J is a very strong function of temperature; it can change many orders of magnitude per degree kelvin near the critical point of a fluid.

To locate the spinoidal curve, one must determine the value of J which characterizes spontaneous homogeneous nucleation. Evidently, this value is very dependent on the physical situation (i.e., the type of superheat experiment) one is dealing with. Presumably, this is due to the success with which one can minimize the degree of heterogeneous nucleation that occurs along with the homogeneous nucleation (Patrick-Yeboah 1979).

ON THE POSSIBILITY OF SHOCK FORMATION

A. Brief Introduction to Shock Wave Theory

Consider a flat piston which moves into a gas with a constant velocity. If the resulting disturbance caused by the piston is weak, i.e., the peak pressure is not much greater than ambient, the compression wave will propagate into the gas unchanged with respect to its pressure, density, and velocity profiles. This is because the gasdynamic equations (the equations of continuity, motion, and energy) become essentially linear for weak disturbances. However, stronger disturbances make nonlinear effects important; the result being to make the peaks (maxima) of the waves travel faster than the valleys (minima), which leads to solutions for the velocity profiles that are not unique (Zeldovich and Raizer 1968) (Figure 5).

In order to remove this uniqueness problem, discontinuous solutions were used. In reality, very thin regions develop which contain very steep gradients, as opposed to discontinuities, in the fluid's properties, e.g., velocity, pressure, density, and temperature. These are known as shock waves.

In order to approximate the thin shock layer by a discontinuity, one must neglect intermolecular interactions, such as heat transfer and momentum transfer from viscous effects, in addition to the molecules' physical dimensions. An order of magnitude analysis of the stresses in the shock layer indicates that its thickness will be the same magnitude as the molecular mean free path, which is much smaller than any flow dimension (Shapiro 1953). So, even though these assumptions restrict any attempts to gain detailed knowledge of the shock layer, they will not hinder the determination of the shock's effect on the gases which pass through it. By

defining variables before and after the shock in terms of a coordinate system that moves with the shock (Figure 6), the equations governing shocks are:

Continuity $$\rho_1 u_1 = \rho_0 u_0 \quad (10a)$$

Conservation of momentum $$P_1 + \rho_1 u_1^2 = P_0 + \rho_0 u_0^2 \quad (10b)$$

Conservation of energy $$h_1 + \frac{1}{2} u_1^2 = h_0 + \frac{1}{2} u_0^2 \quad (10c)$$

where ρ = density

u = velocity relative to the moving shock

P = pressure

h = enthalpy

Assuming that $h(\rho,P)$ is available from an equation of state, and that ρ_0 and P_0 are known, information regarding the strength of the shock wave (P_1 or u_0-u_1) is needed to solve the conservation equations for the remaining variables. By eliminating u_0 and u_1 from the conservation equations, the Hugoniot relation can be obtained:

$$h_1 - h_0 = \frac{1}{2} (P_1 - P_0) \left(\frac{1}{\rho_0} + \frac{1}{\rho_1}\right) \quad (11)$$

From (11), the Hugoniot curve (also known as the Rankine-Hugoniot curve) is obtained: $P_1 = H(P_0,\rho_0,\rho_1)$. For an ideal gas with constant heat capacities, C_p and C_v, the Hugoniot curve is :

$$\frac{P_1}{P_0} = \frac{\left(\frac{\gamma+1}{\gamma-1}\right)\frac{\rho_1}{\rho_0} - 1}{\left(\frac{\gamma+1}{\gamma-1}\right) - \frac{\rho_1}{\rho_0}}$$

where $\gamma = C_p/C_v$. Note that as ρ_1/ρ_0 approaches a finite limit, $(\gamma+1)/(\gamma-1)$,

P_1/P_0 aproaches infinity. At high pressures and temperatures, γ is no longer constant, but the density ratio still remains finite being usually no larger than approximately 13 (Zeldovich and Raizer 1968).

Other relationships that have been developed, but have limited use, are the Fanno line and the Rayleigh line. The Fanno line represents the locus of states after a shock that are associated with a particular state before the shock which are obtainable by solution of the continuity and energy equations, and with $h(\rho,P)$, but not the momentum equation. The Rayleigh line is identical to the Fanno line in concept, except the momentum equation is used and the energy equation is excluded. Of course, any real state must lie at the intersection of the Fanno and Rayleigh lines.

If the piston has a finite acceleration, rather than a constant velocity, compression waves of increasing strength will be created that propagate from the piston. Eventually all of these waves will combine to form one shock front that will eventually reach a maximum velocity.

Studies of shock formation are often performed in shock tubes (Rothkopf and Low 1976), which consist of high pressure and low pressure sections of straight tubing separated by a diaphragm. As the diaphragm is opened (or is allowed to disintegrate), the high pressure gas flows into the low pressure section with subsequent shock wave formation downstream from the diaphragm. It has been shown that the "shock formation distance", defined as the distance from the diaphragm at which the shock reaches its maximum velocity, is directly proportional to the maximum shock velocity (which is also a measure of the shock's strength) and to the diaphragm opening time. The diaphragm opening time is related to the acceleration of the high pressure gas "piston" that moves into the low pressure gas, i.e., the faster the diaphragm is opened, the greater the acceleration will be and

the closer to the "piston" the shock will be. The diaphragm opening time is usually on the order of 0.5 milliseconds.

B. Characteristic times involved in depressurization explosions

For a depressurization explosion, there are three impulses that may lead to shock wave formation. The first is the pressure blow-down itself; the acceleration of the high pressure gas that exits the vessel may send out a shock wave whose strength will be directly proportional to the gauge pressure within the vessel prior to venting. The second is the impulse sent out if the liquid expands explosively due to rapid homogeneous nucleation. The third is the possibility that the rapid growth of any bubble in a superheated liquid is the expansion that leads to shock formation. It is possible that if two or more of the above processes create shocks, they could combine to form one stronger shock at a small distance from the ruptured vessel provided that the time lags between the separate shock creations are not too great.

Of course, the mode of depressurization will affect the liquid's thermodynamic path during depressurization which will affect the possibility of homogeneous nucleation. If the depressurization is slow, the depressurization itself will not create a shock wave; in addition, the liquid will expand slowly allowing time for heat to transfer from the surroundings to the fluid. Bubbles, created from boiling on the vessel walls, will disperse throughout the liquid. The bubbles then become heterogeneous nucleation sites in the bulk liquid, thereby decreasing the probability of obtaining the superheat necessary for explosion. For a fast depressurizationthe depressurization itself will cause a shock; also, the liquid will be allowed to superheat to a great extent due to the lack of time

for heat transfer to take place.

In order to assess the relative importance of these various phenomenon, a comparison of characteristic times for five processes will be beneficial: for depressurization, homogeneous nucleation, bubble growth, a bubble rising into the bulk superheated liquid, and heat transfer from the surroundings.

For those processes that may disturb the bulk liquid, the characteristic times should reflect the time it takes for such a process to significantly alter the bulk's conditions. And for those processes that may create shocks, the characteristic times should reflect the time that it takes the process to create an impulse that might drive an explosion.

Rising Bubbles

If we assume that a depressurizing mass of liquid experiences disturbances at its boundaries (walls or free surfaces), then an undisturbed bulk will exist only near the middle of the liquid. So, bubbles will have completely disturbed the bulk liquid when they reach the middle of the liquid. If we take the depth of the liquid to be "h", the characteristic time for bubbles to disturb the bulk, τ_B, can be defined as the time it takes a bubble to rise from the bottom ($z = 0$) to the middle ($z = h/2$). As a first approximation consider a small spherical bubble of constant radius, R, rising with velocity, v, due to buoyancy forces alone in a liquid of constant temperature; furthermore, internal motion is ignored so that a force balance on the bubble is given by:

$$m_B \, v \, \frac{dv}{dz} = \frac{4}{3} \pi R^3 \rho_L \, g - 6\pi\mu \, R \, v \qquad (13)$$

where m_B is the mass of the bubble ($= 4\pi R^3 \rho_G/3$), ρ_G and ρ_L are densities of vapor and liquid, and μ is the viscosity of the liquid, g is the acceleration due to gravity. From these assumptions, (13) can be integrated directly to give:

$$\ln\left(1 - \frac{Bv}{A}\right) + \frac{Bv}{A} = -\frac{B^2 z}{A} \qquad (14)$$

where $A = \rho_L\, g/\rho_G$ and $B = 9\mu/2R^2\rho_G$.

The velocity will approach a terminal velocity of A/B, as expected. And from the velocity profile, τ_B, can be calculated from:

$$\tau_B = \int_0^{h/2} \frac{dz}{v(z)} \qquad (15)$$

Due to the implicit nature of the solution for v(z), this integral must be evaluated graphically or numerically; since the velocity will vary as $z^{1/2}$ as z approaches zero, the integral in (15) is not singular.

Of course, this is a very naive approximation. Many of the assumptions are not valid for a bubble in a liquid that is superheating. The greatest discrepancy is the fact that the bubble will grow quite rapidly, as will be seen in the discussion of bubble growth. But as the bubble gets larger, its shape will deviate from spherical, accompanied by oscillations, which gives velocities much smaller than for a solid sphere model (Perry and Chilton 1973).

Some effects will serve to increase the bubble's velocity, e.g., the bubble will expand due to decreases in hydrostatic pressure as it rises. Others will serve to decrease bubble velocity, e.g., temperature decreases will decrease ρ_L/ρ_G.

Due to the balancing of many forces on the bubble, the use of (15) from this simple model may be valid only for order of magnitude estimates.

Heat Transfer

As depressurization occurs, the liquid's temperature profile will be influenced by three aspects of the heat transfer: (a) the bulk temperature will be decreasing as the liquid expands isentropically far from the vessel walls (this is evident from Figures 3 and 4), (b) the wall's high heat capacity will make the temperature constant at the wall, and (c) boiling at the wall will serve to increase temperature gradients in the wall's vicinity. From these conjectures, the expected temperature profile will be as in Figure 7. In reality, this is a penetration theory problem with a time-dependent boundary condition. To simplify the analysis, it will be assumedthat all of the heat transfer occurs within a fixed distance, L, from the wall (Figure 8). Physically, $x = L$ is the middle of the bulk liquid.

The mathematical statement of this simplified problem is given by:

$$\frac{\partial T}{\partial t} = \alpha \frac{\partial^2 T}{\partial x^2}$$

$$t = 0: \quad T = T_0$$
$$x = 0: \quad T = T_{wall} = T_0$$
$$x = L: \quad T = T_b(t), \quad T_b(0) = T_0$$

where $T_b(t)$ is the bulk temperature, which can be related to the rate of depressurization by:

$$\left(\frac{dT_b}{dt}\right)_s = \left(\frac{dT_b}{dP}\right)_s \left(\frac{dP}{dt}\right)_s = -\beta \qquad (16)$$

From Figures 3 and 4, $(dP/dT)_s$ is approximately constant, so for a constant depressurization rate, β will be approximately constant. So, $T_b = T_0 - \beta t$.

Defining dimensionless temperature, time, and distance by $\theta = (T-T_0)/T_0$, $\xi = \alpha t/L^2$, and $\eta = x/L$, respectively, the problem becomes :

$$\frac{\partial\theta}{\partial\xi} = \frac{\partial^2\theta}{\partial\eta^2} \qquad \xi = 0: \quad \theta = 0$$
$$\eta = 0: \quad \theta = 0$$
$$\eta = 1: \quad \theta = -B\xi$$

where $B = \beta L^2/\alpha T_0$.

Solution by Duhamel's superposition method (Arpaci 1966; Appendix III) gives:

$$\theta = -B\left[\eta\xi + 2\sum_{n=1}^{\infty}\frac{(-1)^n}{(n\pi)^3}\sin n\pi\eta\ (1 - e^{-n^2\pi^2\xi})\right] \quad (17)$$

From this, the characteristic time for heat to disturb the bulk liquid, τ_H, can be defined as the time it takes for the rate of temperature change of the bulk liquid due to heat flux alone, denoted by dT_H/dt, to be equal to some appreciable fraction, F, of the rate of temperature change of the bulk liquid due to the isentropic expansion alone given by (16). Quantitatively, for a heat flux q:

$$\frac{dT_H}{dt} = \left(\frac{q}{L\,\rho C_p}\right)_{x=L} = -\frac{\alpha T_0}{L^2}\left(\frac{\partial\theta}{\partial\eta}\right)_{\eta=1}$$

and the criterion for τ_H (or $\xi_H = \alpha\tau_H/L^2$) is :

$$\left|\left(\frac{\partial\theta}{\partial\eta}\right)_{\substack{\eta=1\\ \xi=\xi_H}}\right| = BF \quad (18)$$

Evaluating the derivative in (18) from (17) gives:

$$\left|\xi_H + 2\sum_{n=1}^{\infty}\frac{(1 - e^{-n^2\pi^2\xi_H})}{n^2\pi^2}\right| = F$$

The following table gives ξ_H as a function of F.

F	0.0	0.1	0.2	0.3	0.4	0.5	0.6	0.7	0.8	0.9	1.0
ξ_H	0.0	.0081	.032	.071	.13	.20	.28	.37	.47	.57	.67

Typical values for a CO_2 or propane tank car are L = 300 cm (10 ft), $\alpha = 10^{-4}$ $cm^2 s^{-1}$, so for the temperature change rate to be reduced by ten percent (F = 0.1), it will take approximately 7.3×10^6 seconds.

So, this model indicates that direct heat transfer disturbances will be negligible. However, if boiling is initiated on the walls early during the depressurization, then boiling will become more pronounced as time progresses, since the driving force for heat transfer from the wall to the liquid, $T_{wall} - T_b(t)$, will increase. In essence, heat transfer from the liquid's surroundings to the liquid will not hinder attempts to superheat the liquid by rapid depressurization unless boiling occurs to create bubbles which will disrupt the bulk superheated liquid.

Depressurization

The force that creates the shock-forming impulse in depressurization is the pressure, P, so the characteristic time for this impulse can be defined by:

$$\tau_D = \left(\frac{1}{P}\frac{dP}{dt}\right)^{-1} \tag{19}$$

Nucleation

The impulse from nucleation is the expansion due to the sudden vaporization of the liquid. With a knowledge of J, the nucleation rate, the characteristic time for nucleation can be obtained. Consider a critical bubble of volume $4\pi r_c^3/3$ filled with a vapor of density ρ_G that grew from a volume of liquid, $\underline{V}_L$, of density ρ_L which contains the same number of molecules as in the bubble, i.e., $\frac{4}{3}\pi r_c^3 \rho_G = \underline{V}_L \rho_L$. The average time it takes for this process to occur is the characteristic time for nucleation, τ_N, which is given by:

$$\tau_N = (J\,\underline{V}_L)^{-1} = \frac{\rho_L}{\rho_G}\,\frac{1}{\frac{4\pi r_c^3}{3} J} \tag{20}$$

Skripov (1974) gives a definition for τ_N very similar to (20), but it is based on the total volume of superheated liquid available rather than the volume to create one bubble; the present analysis assumes that the whole mass of superheated liquid will nucleate at once, while Skripov's analysis inherently assumes that the nucleation occurs one bubble at a time.

To apply (20) to depressurization explosions, it must be assumed that the expression for J is still valid for physical properties (e.g., P, T, σ, etc.) that are varying with time, and that nucleation occurs only at a fixed point during the depressurization (e.g., on the spinoidal curve).

Strictly speaking, the derivation of J assumes that nucleation occurs anytime that a superheated liquid is formed. So, if nucleation is occuring throughout the depressurization, then it will not be J which creates the expansion impulse; the impulse will be created by increases in J, i.e., dJ/dt. Taking this to be a "force" analogous to pressure in (19), a new

characteristic time, τ_N^*, can be defined for this dynamic model:

$$\tau_N^* = \left[\frac{1}{(dJ/dt)_s} \frac{d}{dt}\left(\frac{dJ}{dt}\right)_s \right]^{-1} \tag{21}$$

where the derivatives are evaluated on isentropic paths. τ_N^* can be related to τ_D by rewriting the time derivatives as:

$$\frac{dX}{dt} = \frac{dX}{dP}\frac{dP}{dt} = -\frac{dX}{dP}\frac{P}{\tau_D}$$

Here use of (19) has been used. Substitution of this into (21) gives:

$$\tau_N^* = -\tau_D\left(\frac{dJ}{dP}\right)_s \left[\frac{d}{dP}\left(P\frac{dJ}{dP}\right)_s \right]^{-1} \tag{22}$$

To obtain numerical values for τ_N^* and τ_N, the isentropic path for carbon dioxide that passes through the saturation curve at 298.4 K, 64.8 bar was considered (See table 1). The Peng-Robinson equation of state was used and it was assumed that the surface tension for a superheated liquid is the same as that for a saturated liquid at the same temperature. Grigull and Straub (1969) have reported surface tensions for saturated liquid CO_2 over a wide range of temperatures.

As Table 1 indicates, τ_N is on the order of microseconds near the spinoidal curve even for the small superheat considered (< 10 K). Because J is such a strong function of temperature, the evaluation of the derivatives in (22) are quite difficult; a three-point finite difference interpolation scheme (Abramowitz and Stegun 1974) was used, but note that this scheme gives the wrong sign at 292 K for $d\log_{10}J/dT$. However, if we assume that the middle point at 294 K is valid for an order of magnitude estimate, then:

$$\left(\frac{dJ}{dP}\right)_s \sim \left(\frac{dJ}{dT}\right)_s \left(\frac{dT}{dP}\right)_s \sim -0.193 \text{ J, cm}^{-3}\text{s}^{-1}\text{atm}^{-1}$$

Use of this in (22) gives:

$$\tau_N^* \sim -\frac{\tau_D J}{\frac{d(PJ)}{dP}} \sim \frac{\tau_D}{0.193P - 1}$$

Since $P \sim 50$ bar, then $\tau_N^* \sim 0.1\ \tau_D$.

Bubble Growth

Using the accelerating piston analogy for shock formation, the impulse from bubble growth will be related to the speed at which the vapor pushes against the liquid, i.e., the velocity of the vapor-liquid interface, which is just dR/dt for a spherical bubble. Hence, the characteristic time for impulses due to bubble growth, τ_G, can be defined by:

$$\tau_G = \frac{dR}{dt}\left(\frac{d^2R}{dt^2}\right)^{-1} \qquad (23)$$

There are four stages in the growth of a bubble surrounded by superheated liquid: the initial, or latent, stage after the critical bubble has formed where surface tension is the main hindrance to growth, after which comes the inertial stage where the inertia of the liquid is the predominant limitation, followed by an intermediate stage where thermal effects (i.e., limitations due to finite heat transfer for vaporization of liquid) become comparable to inertial effects, and finally the asymptotic stage where thermal effects are predominant. In regards to shock formation, the strongest impulses sent out by a growing bubble will occur during stages

where inertial effects are important, namely the inertial and intermediate stages, because at these times the liquid is being rapidly compressed. Quantitatively, we would expect that these will be regions where the acceleration of the liquid-vapor interface, d^2R/dt^2, is large.

By solving the Rayleigh and energy equations, Prosperetti and Plesset (1978) have obtained expressions for R(t) in superheated sodium during all but the latent stages. Their results indicate that d^2R/dt^2 is largest during the inertial stage, and that dR/dt is greatest during the transition between the inertial and intermediate stages. But, their results also show that the inertial stage is reached only for large superheats ($\sim$100 K). For small superheats ($\sim$ 1 to 10 K) the latent stage passes directly to the intermediate or asymptotic stage.

For a wide range of superheats, 4.66 to 340.1 K, and for low pressures, 0.5 to 6 atm, their calculations for bubble growth as a function of time indicate that:

$$\tau_G = c\, t_I \tag{24}$$

where t_I is the time it takes to reach the inertial stage and c is a constant of order unity. For liquid sodium, τ_G is on the order of one microsecond for small superheats and can be on the order of 10^{-2} microseconds for large superheats.

For liquids other than sodium, Prosperetti and Plesset's analysis should be repeated for a confident estimate of τ_G. However, bubble growth rates during the inertial stages are dependent mainly on pressures and liquid densities, so liquids that experience similar densities and pressures upon superheating will have values of τ_G that are of the same magnitude.

So, for the previous superheated CO_2 depressurization, it would be expected that τ_G is of order 1 μs at 294 K. This is comparable with τ_N.

CRITERIA FOR SHOCK

When a flame-related explosion occurs, the mechanism usually involves the creation of atoms or free radicals that react to create even more active intermediates, causing the reaction rate to increase exponentially with time. The reaction times for these combustion processes vary from one second to less than one microsecond.

In a detonation, a reaction zone, which is a strong shock, passes through the explosive. To sustain the detonation, the reaction rate must be fast enough to complete the reaction within the reaction zone. For nitroglycerin, the reaction time is on the order of 0.1 microseconds or less (Tedder et al. 1975).

If it is assumed that the impulses due to depressurization, nucleation, and bubble growth are similar to explosions, it would be expected that τ_D, τ_N, τ_N^*, and/or τ_G are the same order of magnitude as the reaction times for chemical explosives.

From this criterion for explosion, all four processes mentioned can produce shocks. By analogy with shock tube experiments, if τ_D is equal to the diaphragm opening time then shock will certainly occur from the blowdown itself; the diaphragm opening time is of order 1 ms, which is within the reaction time scales. As was shown earlier, τ_N and τ_G are of order 1 μs, so nucleation and bubble growth may both be mechanisms for detonations. Also, $\tau_N^* \sim 0.1\ \tau_D \sim 0.1$ ms, so "dynamic nucleation" could cause shock.

In addition, it would be expected that the smaller the characteristic time, the stronger the shock will be, since the shorter time scales will generally correspond to greater accelerations. This criterion and information from Table 1 indicates that the greater the superheat the stronger the

shock, as might be anticipated.

Processes that will inhibit shock formation must have characteristic times that are much greater than the characteristic times for shock-creating processes if shock is to occur. So one more criterion for shock is $\tau_B, \tau_H >> \tau_N, \tau_N^*$, or τ_G.

In regards to injury to personnel and structures due to shock waves, it is not enough to just examine criterion for shock formation alone. Knowledge of shock propagation must also be included, since the peak pressure's duration as well as its magnitude is important in determining the hazard potential of depressurization explosions.

However, nucleation and bubble growth could produce strong shocks with long duration provided that there is sufficient superheat and liquid mass to sustain the detonation.

EXPERIMENTAL APPARATUS AND PROCEDURE

Figure 9 presents a block diagram of the experimental apparatus and instrumentation used to study depressurization explosions. Figure 10 shows details of the liquid-holding container. Carbon dioxide was chosen as the test fluid for safety reasons.

Before the liquid CO_2 is introduced into the holding container, the container was flushed with CO_2 gas at a pressure of 120 psig by pressurizing then venting the container three times to remove air from the system. And to prevent flashing of the liquid to form dry ice that might clog the filling lines, the CO_2 gas was also used to initially pressurize the container to 120 psig, which is well above the triple point pressure of CO_2.

To hasten the filling process, the container was cooled by pumping cold antifreeze (60/40, by volume, ethylene glycol - water mixture) through the container's jacket. Chunks of dry ice were added directly into the tank to cool the antifreeze to approximately $-10^{o}C$. By placing the eductor-equipped CO_2 cylinder on a scale, the mass of liquid that entered the container could be measured directly. From this and measurement of pressure, the volume fraction of liquid in the container can be calculated (Appendix IV).

In order to heat the liquid to the desired saturated or supercritical state before depressurization, the container was heated by pumping warm antifreeze through the jacket or by using a heating tape. To heat the antifreeze from $-10^{o}C$, a large heating elementwas placed directly into the cold antifreeze. This heating process was very slow, so the use of a heating tape was preferable.

As the pressure within the container approached the desired value, the

heating tape (or pump) was turned off. On the slower warming trend, the solenoid valve was activated remotely when the desired pressure was finally reached. The solenoid valve allowed the 100 psig nitrogen gas to enter the pneumatic cylinder which drove the plunger into the burst disc, thus depressurizing the vessel.

The depressurization was monitored by two pressure transducers located on either side of the bust disc head on top of the container. The transducers translated the pressure-time trace into a DC voltage-time trace. As the container's pressure decreased/increased, a quartz crystal in the tip of the transducer expanded/compressed, which created a net depletion/accumulation of charge across a capacitor (also in the transducer). These charge variations were translated into DC voltage signals, which were linearly related to the pressure changes imposed on the crystal (i.e., the transducer). If the pressure were to be constant after a period of fluctuations, the crystal would no longer be generating charge fluctuations, so the capacitor would tend to discharge, leading to a decay of the transducer's output to zero voltage. So, the transducers used in this study cannot give absolute pressures; in fact, if the pressure is steady, or the pressure fluctuations occur on a time scale that is longer than the capacitor's discharge time scale (approximately one second), then the transducer will register zero voltage, i.e., no signal. The transducers' rise times are one microsecond, so very fast pressure changes, such as those anticipated in this study, could be monitored accurately.

Each voltage signal from the transducers is sent to an electronic signal recorder; the model used was a tape recorder with fast writing, high resolution capabilities. A twenty millisecond tape loop continually records and erases itself as it cycles in the "record" mode. When the signal that

the recorder receives from the transducer is of sufficient magnitude on a rising (or falling) slope, the recorder will trigger, capture the signal, then enter the "playback" mode. Both the magnitude and slope parameters are operator adjustable by the "level" dial and slope selection switch, respectively. In addition, there is a delay setting which allows the 20 ms time span of the captured signal to begin anywhere from 0 to 16 ms before triggering occurs. Theoretically, by using different delays on the two recorders, more than just 20 ms of the depressurization may be recorded. In reality, it was very difficult to accomplish this.

The electronic signal recorders were designed to be applied to circuit trouble-shooting: a continuous signal could be fed and, by adjusting the triggering level slowly, but randomly, the desired part of the voltage signal may be captured. For this reason, it was not possible to anticipate the correct trigger level for any given depressurization, simply because no real correspondence to the level setting and the triggering level existed. To ensure that the recorders did trigger, the level adjustment was varied until it triggered to "playback" from "record" without an input signal; at this point, intrinsic noise within the recorder is causing it to trigger. Then by changing the level adjustment just slightly counterclockwise from this point, it was assumed that triggering would occur such that the first 20 ms of the depressurization could be recorded. However, sometimes it worked, sometimes it failed.

Once a signal was captured, the recording could be viewed on an oscilloscope and a photograph taken with an oscilloscope camera.

For safety, the entire container was mounted on a steel frame and bolted to the wall and floor of a cell made of one-inch thick armor-plate steel. The cell was equipped with blast-resistant lights and a high capacity ventilation system.

MODELLING OF THE DEPRESSURIZATION

In order to test the proposed mechanism for depressurization explosions, it will be assumed that:

(a) The fluid in the container expands isentropically.

(b) The pressure is uniform throughout the container.

(c) Flow through the burst disc is the same as flow through a sharp-edged orifice.

(d) No nucleation occurs unless the spinoidal curve is reached.

(e) If the spinoidal curve is reached, homogeneous nucleation will occur in an explosive manner.

From these assumptions, and the anticipated time scales, the expected pressure trace will be as in Figure 11.

To check assumption (c), preliminary blow-down experiments were performed with nitrogen gas at room temperature. For an ideal gas with constant heat capacity, the depressurization will be given by (Appendix V):

$$\frac{P}{P_0} = \left[1 - \frac{C\,A}{\underline{V}} \left(\frac{R_G T_0 \gamma^3}{M} \right)^{1/2} \left(\frac{2}{\gamma+1} \right)^{\frac{(\gamma+1)}{2(\gamma-1)}} \left(\frac{1-\gamma}{2\gamma} \right) t \right]^{\frac{2\gamma}{1-\gamma}} \quad (25)$$

where P_0, T_0 are the initial pressure and temperature, C is the discharge coefficient, A the vent cross-sectional area, $\underline{V}$ the total volume of gas in the container, R_G the gas constant, M the molecular weight, and $\gamma = C_p/C_v$ can be taken as 1.4 for nitrogen gas under the conditions of these experiments.

Figure 12 shows that agreement between data and (25) is good if appropriate values of C are chosen. Ideally, the discharge coefficient should be constant, independent of the initial pressure, but this does not seem to

be the case. Also, the values of C are smaller (by a factor of two or three) than one might anticipate by comparison with results for an orifice in a straight tube.

These discrepancies are probably due to the unusual geometry and obstructions present in the region immediately upstream of the orifice, i.e., the curved contraction leading into the short length of pipe that connects the container to the orifice (burst disc), and the presence of the plunger in the center of the flow. These disturbances to the flow would be expected to result in lower flow rates, hence smaller discharge coefficients, than expected from the simpler flow in a straight tube.

EXPERIMENTAL RESULTS

Figure 13 shows examples of pressure traces from the pressure transducers as observed on an oscilloscope. The high frequency noise superimposed on the traces was always present to some extent and is probably due to shaking during the experiment and/or the transducers not being flush with the inside wall of the container. It was assumed that the actual pressure lies exactly in the middle of the fluctuations. Appendix VI contains data from several experiments in which the CO_2 was initially in a saturated or supercritical state.

In general, agreement between data and the proposed model (assuming an ideal gas with $\gamma = 1.29$ and $C = 0.3$) was poor. Typical results for saturated experiments appear in Figure 14a; the depressurization rate was similar to the model for the first one or two milliseconds, but decayed rapidly after this period. In some cases, the pressure reached a constant (high) pressure or went through a minimum and experienced a short period of pressurization (Runs 5 and 8). This effect is due to a rapid generation of vapor which results from heterogeneous nucleation (i.e., boiling on the container's walls), homogeneous nucleation, or some combination of these. For supercritical fluids, Figure 14b indicates that the assumption of an ideal gas is inadequate, as might be expected. However, the depressurization rate is quite similar to that for a saturated CO_2 experiment: it is fast in the early stages, but slows considerably in later stages. Since the CO_2 will become a liquid as it depressurizes from a supercritical state to the saturation and spinoidal curves, it appears that this vapor formation effect will be a hindrance in reaching the spinoidal curve in supercritical, as

well as saturated, experiments.

In an attempt to minimize this effect, cold antifreeze ($-10^{o}C$) was pumped through the jacket (44 cm^3/s) prior to bursting the disc in some experiments; the pressure was allowed to rise about 10 to 20 psi above the desired pressure, then the antifreeze was pumped through the jacket, and the solenoid was activated when the desired pressure was reached on a cooling trend. Figure 15 shows results for this procedure, which did permit a greater rate of depressurization, but it was still not enough to reach the spinoidal curve.

It is not truly possible to determine trends from this data, since only pressure and the mass of CO_2 are known confidently. Since the container is opaque, it is not possible to detect foaming of the liquid, agitation of the liquid due to pressure pulses or rising bubbles, suspended solid particles that might have inadvertently fallen into the container, etc. In addition, the temperature of the container wall is undoubtedly different than the bulk liquid's temperature, and the magnitude of this temperature difference will be important in characterizing the initial conditions of the experiment, since the temperature difference will affect the degree of boiling on the wall. But accurate measurements of temperature were not possible with the present system; the cooling jacket surrounded the container, thus hindering the measurement of container wall temperatures directly and liquid temperature measurements would require the insertion of thermocouples, which would provide yet another series of nucleation sites.

If it is postulated that boiling on the walls is the only cause of the vapor formation, then saturated experiments with a low initial pressure and a large liquid volume fraction would be expected to give the fastest depressurization rates. A low initial pressure is required, since this

condition needs less heating time to achieve the desired pressure, hence the wall temperature is undoubtedly lower than for experiments carried out at higher initial pressures. And large liquid volume fractions give small vapor volume fractions, which will give rise to fast depressurization rates based on the analysis in Appendix V. (This assumes that the exit of vapor permits the depressurization of the entire system and that the liquid's expansion is negligibly small.)

It is interesting that the experiment that satisfies both of these criteria, Run 7, does exhibit the fastest depressurization. To investigate these two factors, two series of experiments were performed. One series held liquid volume fractionconstant and variedthe initial pressure (which presumably varied the wall temperature); the other series held initial pressure constant and varied the liquid volume fraction. Results are given in Figures 16 and 17, respectively.

For constant initial pressures, larger liquid volume fractions did lead to faster depressurization rates, but only during the first few milliseconds of the depressurization. After this initial stage, the traces seem to be quite unpredictable. This indicates that those factors which will greatly influence the depressurization (e.g., boiling, foaming, etc.) do not appear immediately after depressurization begins.

For constant liquid volume fractions, the effect of varying initial pressure was just as expected with a large liquid volume fraction, so the conjecture that a high initial pressure gave a large wall temperature, which encouraged boiling, seems to be true. But at a smaller liquid volume fraction, there was no effect in the first 1.5 milliseconds of the depressurization and after this period the traces were not as expected. These results are not surprising, though. Boiling is not pronounced in the first one or

two milliseconds of the depressurization, but it will become more violent as time progresses. So, a depressurization involving a small vapor volume (i.e., a large liquid volume fraction) will be affected sooner than one involving a larger vapor volume, simply due to the relation between the boiling rate, the space available to contain the new vapor phase, and the pressurizing that results.

As a final check on this wall-boiling conjecture, a rough estimate of an overall heat transfer coefficient was calculated for Runs 5 and 8 (Appendix VII). The resulting coefficient was approximately 10^5 BTU/hr ft^2 F, which is two orders of magnitude larger than typical heat transfer coefficients (Perry and Chilton, 1973). This indicates that wall boiling is probably not the sole cause of vapor formation.

For supercritical experiments, it was hoped that the spinoidal curve could be reached by using initial states near the critical point. The spinoidal curve was (theoretically) reached in Run 11, but no explosion was observed. Since superheated liquids in the vicinity of the critical point have small degrees of superheat, it is possible that spontaneous nucleation occurred, but in a very weak manner. It is also possible that by the time the system reached the spinoidal curve, the contents of the container were well agitated, so any nucleation that did occur may have taken place on a small scale and, hence, went unnoticed.

Regardless of the initial state, when the burst disc was ruptured, the venting produced a strong pressure wave (possibly a shock) in the cell, accompanied by a loud bang which sounded similar to a rifleshot.

Also, the venting filled the cell with a thick, white plume which lingered for many seconds after the experiment was over. This might indi-

cate that the flow through the burst disc may involve solid and/or liquid phases in addition to a gas phase. When the initial state is saturated, liquid CO_2 might become entrapped in the exit flow and flash to form dry ice mist upon exiting the container. When the initial state is supercritical, the fluid which exits the container will be supercritical or a liquid, both of which may flash to form a dry ice mist.

After experiments with saturated liquids at lower pressures ($\leq$ 650 psig), placing one's hand over the burst disc head causes pressure to build up in the container; this did not occur when the initial conditions were at higher pressures or supercritical. This indicates that at the lower pressures, some dry ice is probably left in the container after the experiment has been completed. Of course, if dry ice forms in the container during the depressurization, this presents yet another obstacle to overcome, since the dry ice particles are excellent nucleation sites.

In all experiments, the burst disc opened completely; in fact, it usually disintegrated to leave a 1.5-inch hole.

CONCLUSIONS

As yet, the full role of superheated liquids in depressurization explosions has not been determined. In particular, the influence of the spinoidal curve, via Reid's model, has not been determined. But,a comparison of estimates of the characteristic times for nucleation and chemical explosives seems to indicate that homogeneous nucleation can be an explosive process.

Obviously, it is not enough just to have a superheated liquid to get a depressurization explosion as the model of Ogiso et al. might suggest. This study did produce superheated liquids to some extent, as indicated by the rapid vapor formation that occurred,but no explosion was observed.

The "quality" of superheat must be important. If the liquid becomes fragmented into many subdivisions which nucleate at very different times, then the sum of their impulses will not likely be an explosion. In addition, the pressure will not necessarily be uniform throughout the vessel. A low-pressure wave will propagate through the liquid after the burst disc is ruptured. This low-pressure wave may act much like a reaction shock zone in explosives; as the wave front passes through the liquid, the pressure drops rapidly in this thin region, creating a localized zone of superheated liquid. Nucleation will occur in this zone, since it occurs on a time scale much shorter than that associated with the wave passing through the liquid. The high pressure vapors that exit the zone might sustain a detonation.

It is possible that the rapid vapor formation resulted from bubbles that were created on solid surfaces, which subsequently detached, then grew rapidly as it rose through the superheated liquid. This process could cause rapid pressure increases in a closed vessel, but would not be expected to cause explosions since bubbles will tend to fragment the bulk liquid.

Of course, this bubble growth mechanism will compete with the "reaction

zone" mechanism, which indicates that a minimum volume of liquid is necessary to insure that wall effects will not disturb the creation of a superheated liquid. The determination of this minimum volume will require the consideration of many processes, such as the influence of rising bubbles on the bulk liquid, heat transfer, etc.

Finally, the initial state of the fluid and the conditions of the venting must be such that a large degree of superheat is attainable in order to get a depressurization explosion. The venting must be rapid even during later stages when there is rapid vapor formation. And, to get large superheats under such venting conditions, the liquid must reach the spinoidal curve (or states near the spinoidal curve) at relatively low pressures. So, the locus of initial states that might lead to depressurization explosions could encompass a rather small region of states.

SUGGESTIONS FOR FUTURE WORK

To successfully obtain a large degree of superheat by depressurizing a liquid, it is necessary to minimize the boiling that occurs on physical boundaries. This can be accomplished by the following:

(a) Use a container that minimizes the surface area-to-volume ratio; this implies the use of a spherical geometry.

(b) Avoid the presence of structures that penetrate into the liquid, e.g., the plunger in this study.

(c) Use the largest vent cross-sectional area possible to effect the fastest depressurization possible.

(d) Coat the inner wall of the container with Teflon, or some other smooth coating, that will serve to reduce roughness, hence, nucleation sites. This could serve a dual purpose in that the coating could also act as an insulating layer that hinders heat transfer from the wall to the liquid.

As mentioned previously, the volume of this apparatus will depend on the depressurization rate that can be achieved. One possible experimental set-up is outlined in Appendix VIII. The proposed set-up will be most manageable on a relatively small scale; if the top can be removed in less than one millisecond, then the scale of the experiment will probably be of no consequence.

Instrumentation should include pressure transducers that give absolute pressures. This will eliminate the need for a pressure gauge, which will allow the experimentalists to be removed from one less high-pressure line.

Wall temperatures should be monitored to get an estimate of the heat

transfer rates into, or out of, the liquid. It is possible to measure the liquid's temperature non-intrusively by using an infrared pyrometer, but this will require a transparent container. It may be difficult to construct a sufficiently strong spherical container using a transparent material such as Lexan or glass, but a window might be installed as an alternative to making the whole container transparent.

Finally, it would be very advantageous to be able to continually record the pressure transducers' signals with a high frequency tape recorder with a long tape,or an oscillograph. This suggestion is motivated by the difficulties experienced with the electronic signal recorders used in this study.

REFERENCES

1. Abramowitz, M. and I.A. Stegun,"Handbook of Mathematical Functions", National Bureau of Standards, 1974
2. Anderson, C., W. Townsend, J. Zook, and G. Cowgill,"The Effects of a Fire Environment on a Rail Tank Car Filled with LPG", USDT, FRA-ORED 75-31, Sept. 1974
3. Angus, S., B. Armstrong, and K.M. deReuck, eds.,"International Thermodynamic Tables of the Fluid State: Carbon Dioxide", compiled for IUPAC, Pergammon Press: New York, 1973
4. Arpaci, V.S.,"Conduction Heat Transfer", Addison-Wesley:Menlo Park,1966
5. Beegle, B.L., M. Modell, and R.C. Reid, AIChEJ, 20, 1194 (1974)
6. Beegle, B.L., M. Modell, and R.C. Reid, AIChEJ, 20, 1200 (1974)
7. Blander, M. and J.L. Katz, AIChEJ, 21, 833 (1975)
8. Burghard, H. and R.B. Wangler,"Physical Failure of a CO_2 Cylinder", personal communication with R.C. Reid, 1979
9. Copeland, E.H.,"Pressure Safety Aspects of Liquid CO_2 Storage - A Case History", Sandia Lab Report, SAND-77-0125, 1976
10. Davidson, N.,"Statistical Mechanics", McGraw Hill:New York, 1962
11. Grigull, U. and J. Straub, Progress in Heat and Mass Transfer,2,151(1969)
12. Leiber, C.O., personal communication with R.C. Reid, 1979
13. Modell, M. and R.C. Reid,"Thermodynamics and Its Applications", Prentice-Hall,Inc.:New Jersey, 1974
14. Moore, G.R., AIChEJ, 5, 458 (1959)
15. Ogiso, C., N. Takagi, and T. Kitigawa,"On the Mechanism of Vapor Explosion", paper presented at PACHEC, Japan (1972)
16. Patrick-Yeboah, J.R., Sc.D. Thesis, Department of Chemical Engineering, Massachusetts Institute of Technology, 1979

17. Peng, D.Y. and D.B. Robinson, Ind.Eng.Chem.Fund., 15, 59 (1976)

18. Perry, R.H. and C.H. Chilton,"Chemical Engineer's Handbook, Fifth Edition", McGraw-Hill:New York, 1973

19. Prosperetti, A. and M.S. Plesset, JFM, 85, 349 (1978)

20. Reid, R.C., Science, 203, 1263 (1979)

21. Reid, R.C., J.M. Prausnitz, and T.K.Sherwood,"The Properties of Gases and Liquids", McGraw-Hill:New York, 1977

22. Rothkopf, E.M. and W. Low, Phys. Fluids, 19, 1885 (1976)

23. Shapiro, A.H.,"The Dynamics and Thermodynamics of Compressible Fluid Flow", Ronald Press:New York, 1954

24. Skripov, V.P.,"Metastable Liquids", Wiley:New York, 1974

25. Takagi, S., J.Appl.Phys., 24, 1453 (1953)

26. Tedder, J.M., A. Nechvatal, and A.H. Jubb,"Basic Organic Chemistry. Part 5: Industrial Products", Wiley:New York, 1975

27. Zeldovich, Y.B. and Y.P. Raizer,"Elements of Gasdynamics and the Classical Theory of Shock Waves", Academic Press:New York, 1968

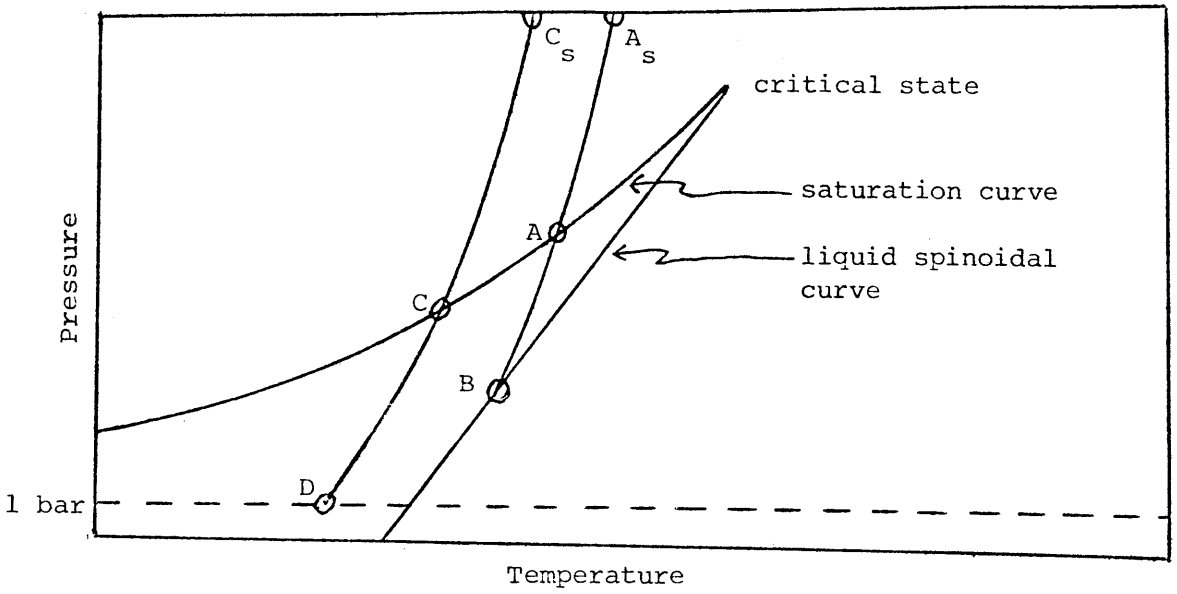

Figure 1

P-T Diagram for a Pure Fluid

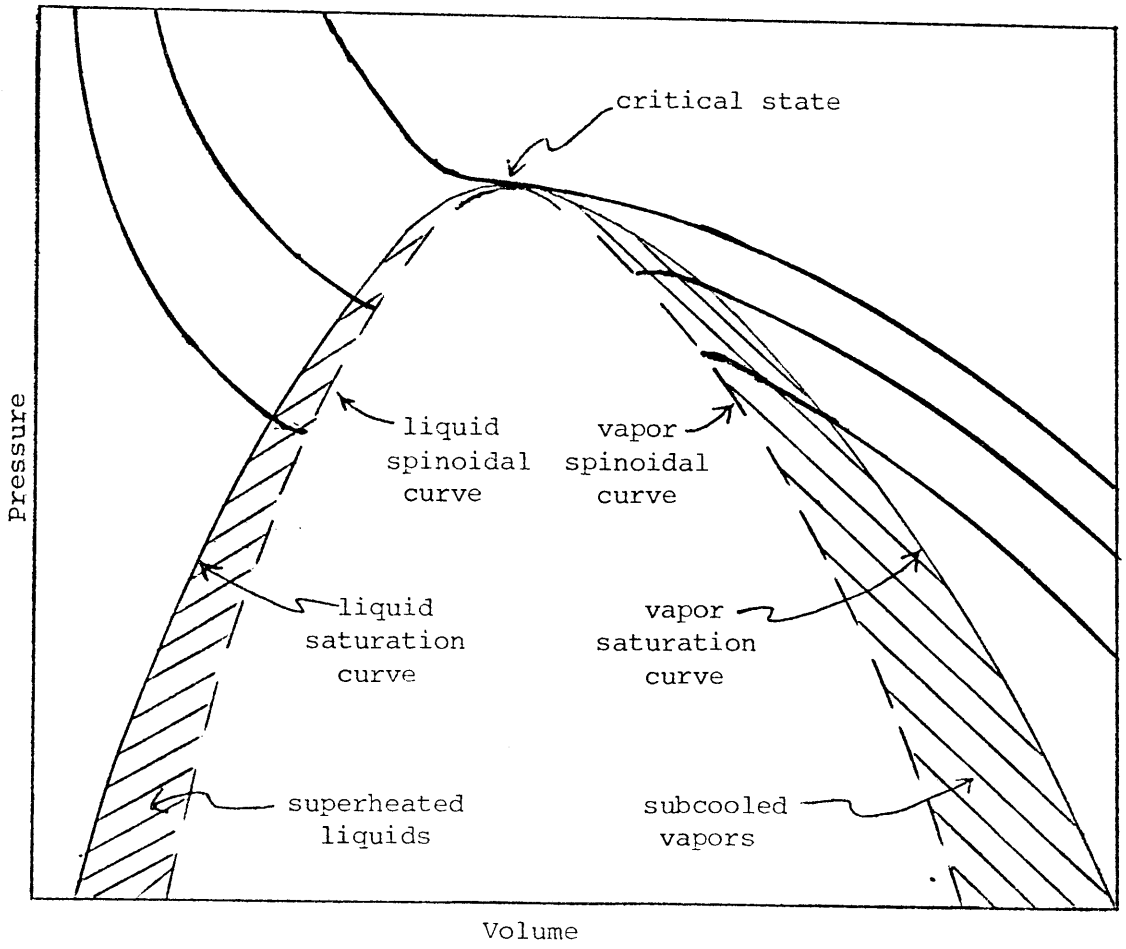

Figure 2

P-V Diagram for a Pure Fluid

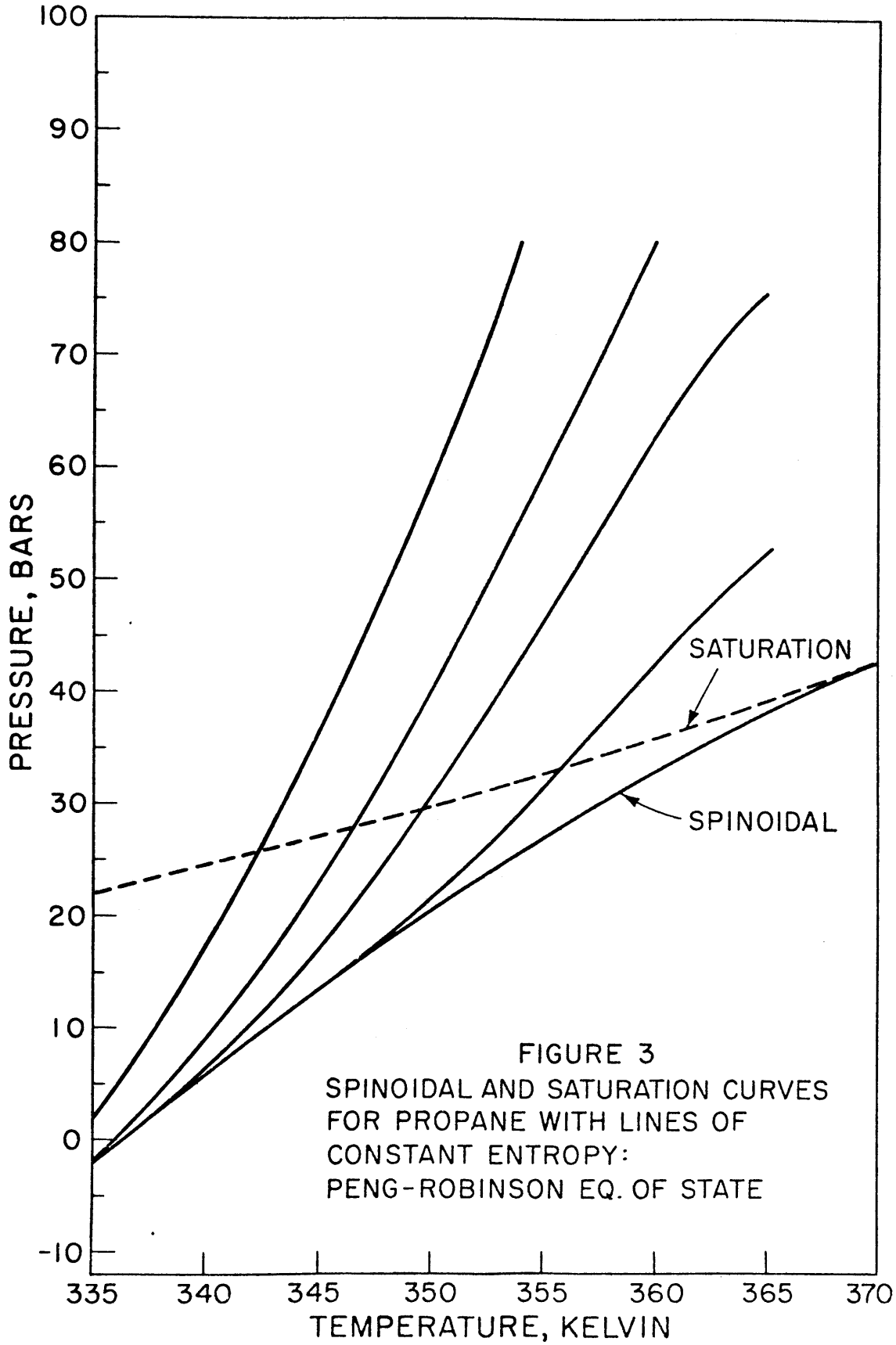

FIGURE 3
SPINOIDAL AND SATURATION CURVES FOR PROPANE WITH LINES OF CONSTANT ENTROPY: PENG-ROBINSON EQ. OF STATE

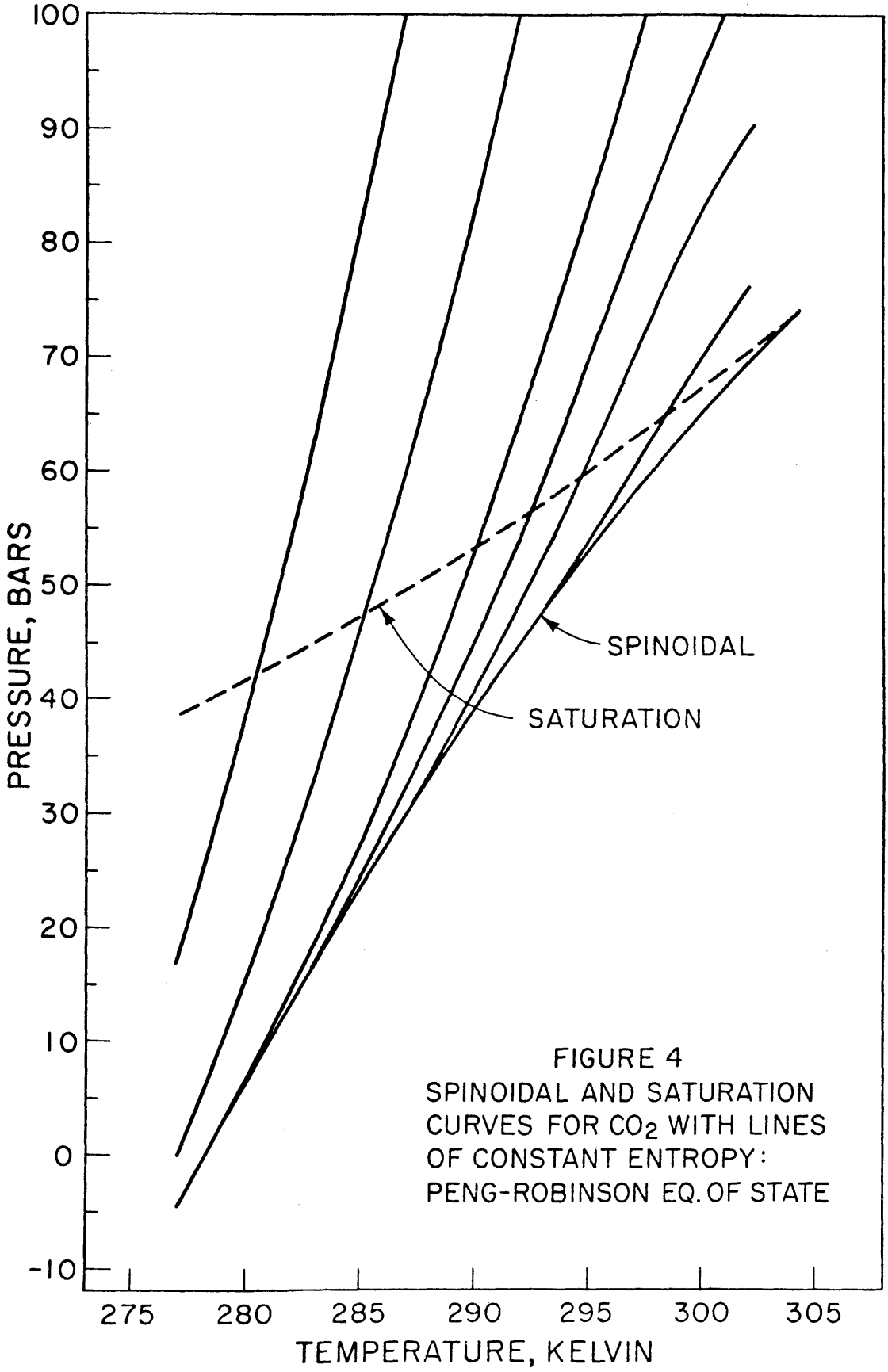

FIGURE 4
SPINOIDAL AND SATURATION CURVES FOR CO_2 WITH LINES OF CONSTANT ENTROPY: PENG-ROBINSON EQ. OF STATE

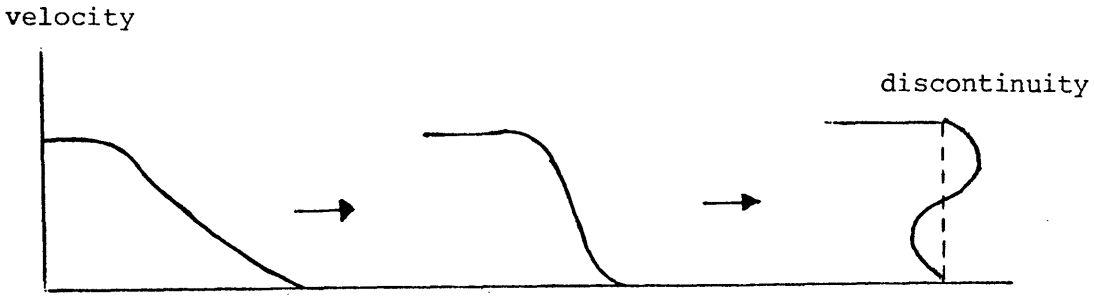

Figure 5

Distortion of a Compression Wave

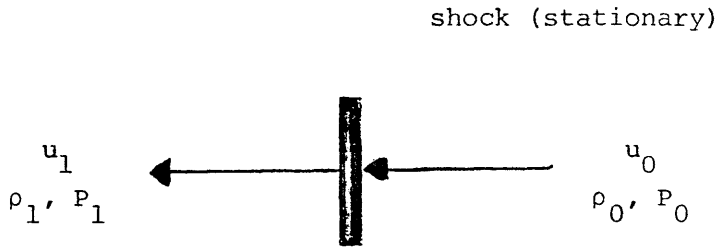

Figure 6

Flow Through a Shock in a Coordinate System Moving with the Shock

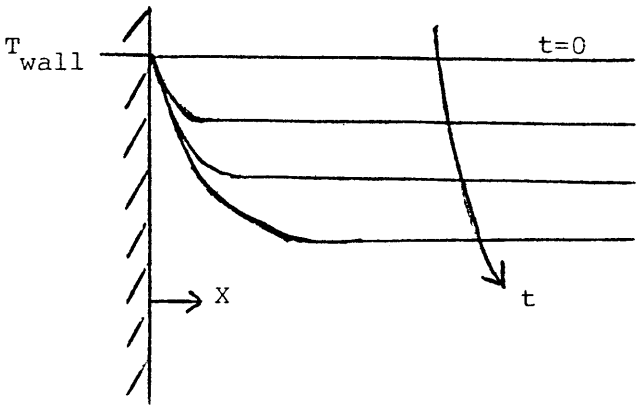

Figure 7

Expected Temperature Profile
During Depressurization

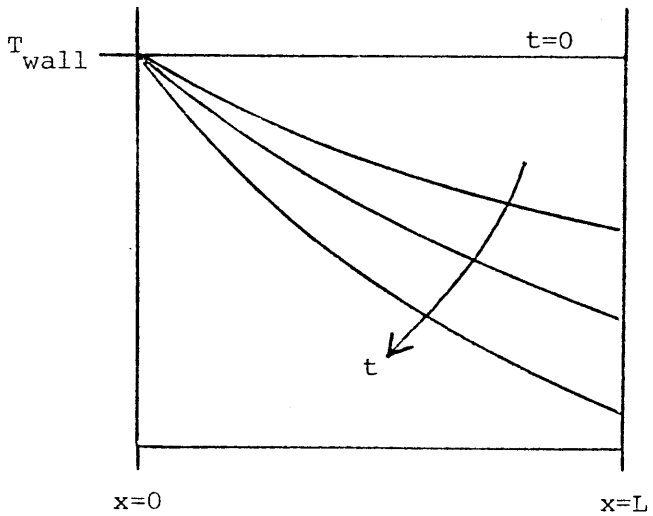

Figure 8

Simplified Model of Heat Transfer

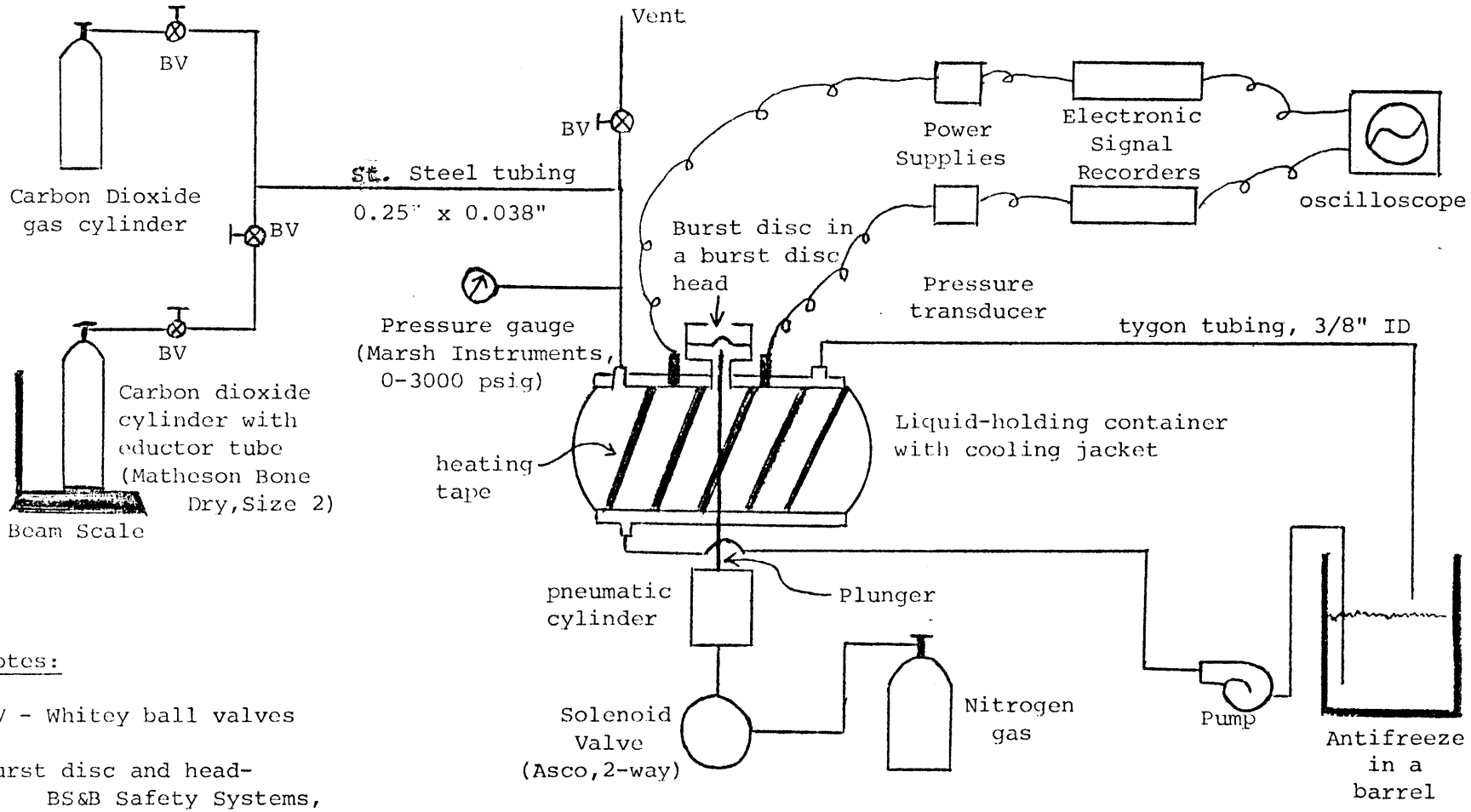

Notes:

BV - Whitey ball valves

Burst disc and head-
BS&B Safety Systems,
1.5" Type B

Electronic Signal Recorders-
Ballantine model 7050A

Pressure transducers-
PCB Piezotronics
models 102A11 and 102A04(kits)

Figure 9

Experimental Apparatus

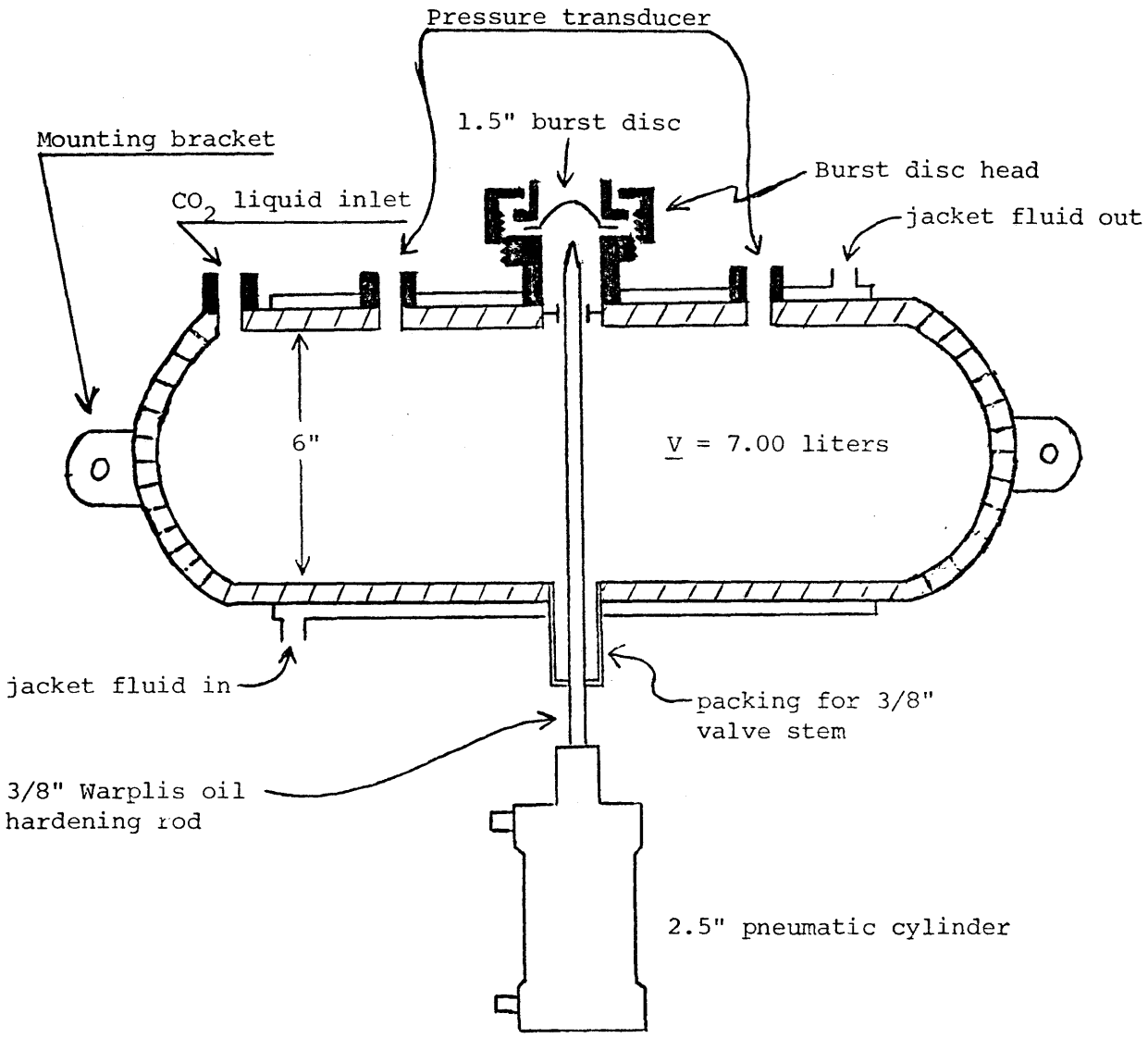

Figure 10

Details of the

Liquid-Holding Container

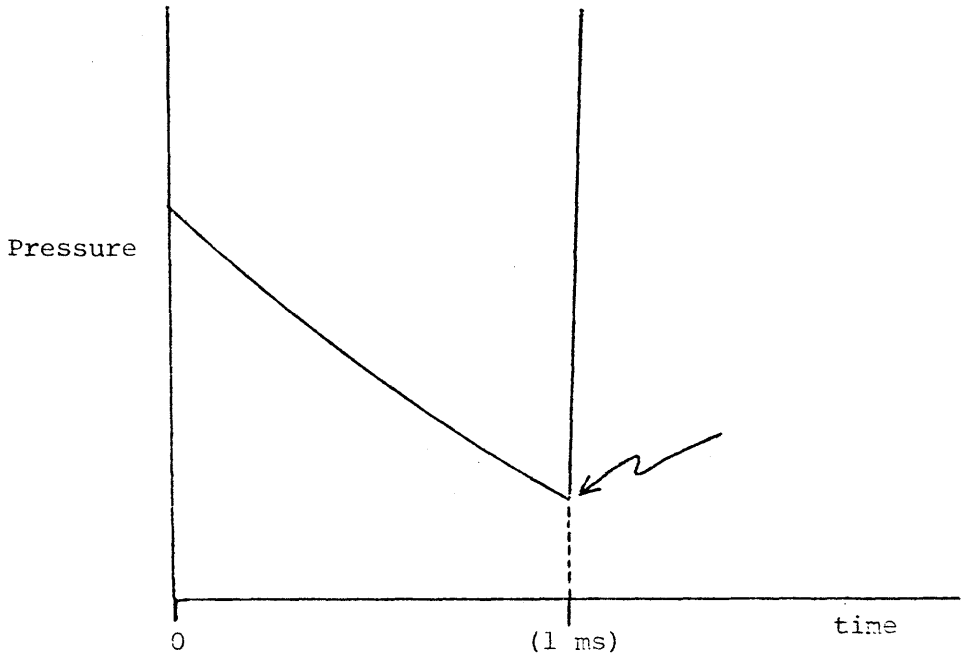

Figure 11

Expected Pressure Trace for a
Depressurization Explosion

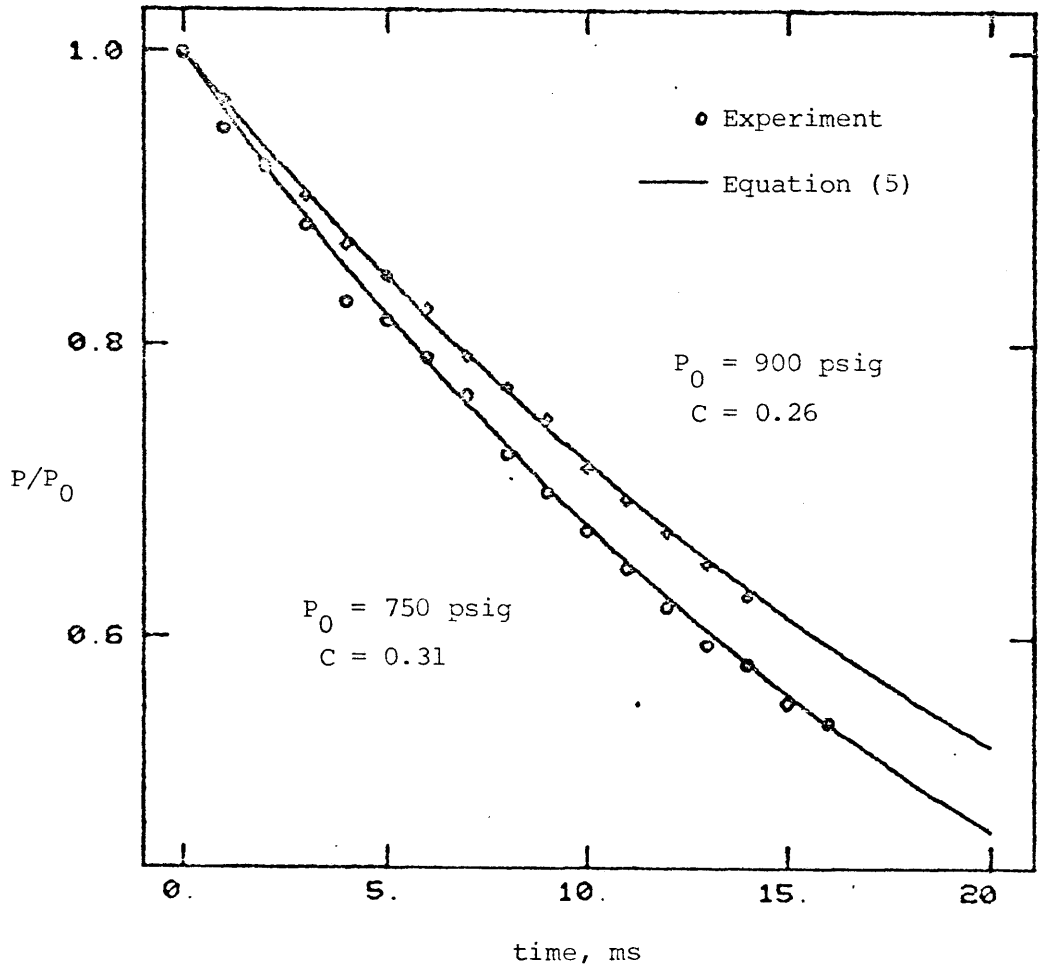

Figure 12

Blow-down Experiments with N_2 Gas

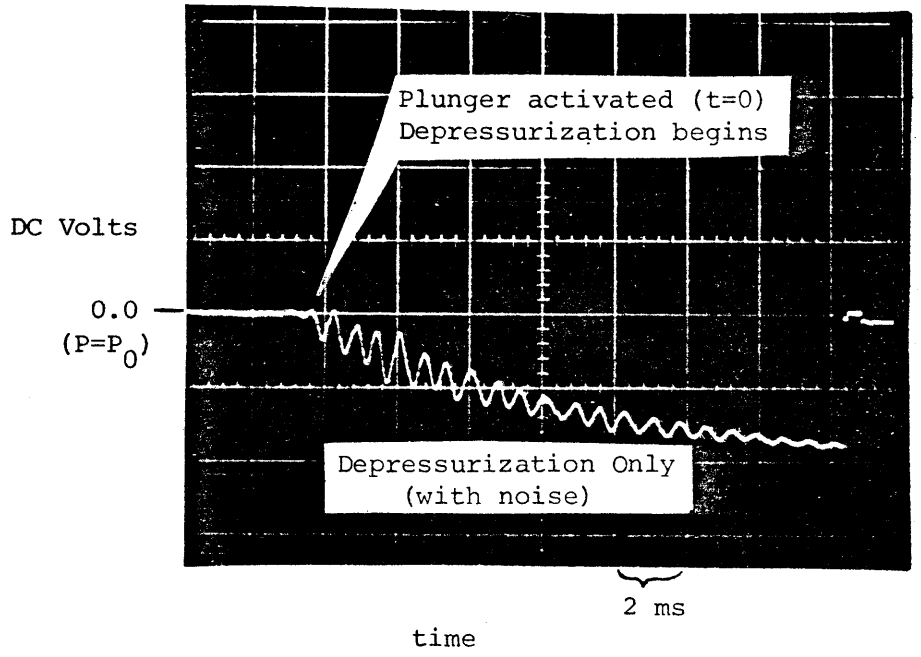

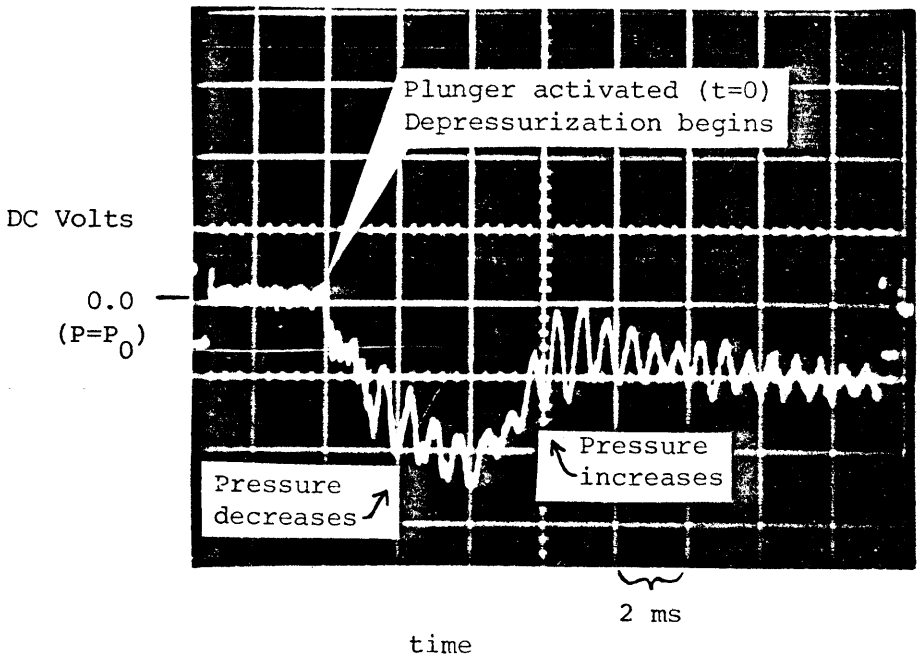

Figure 13

Examples of Pressure Traces

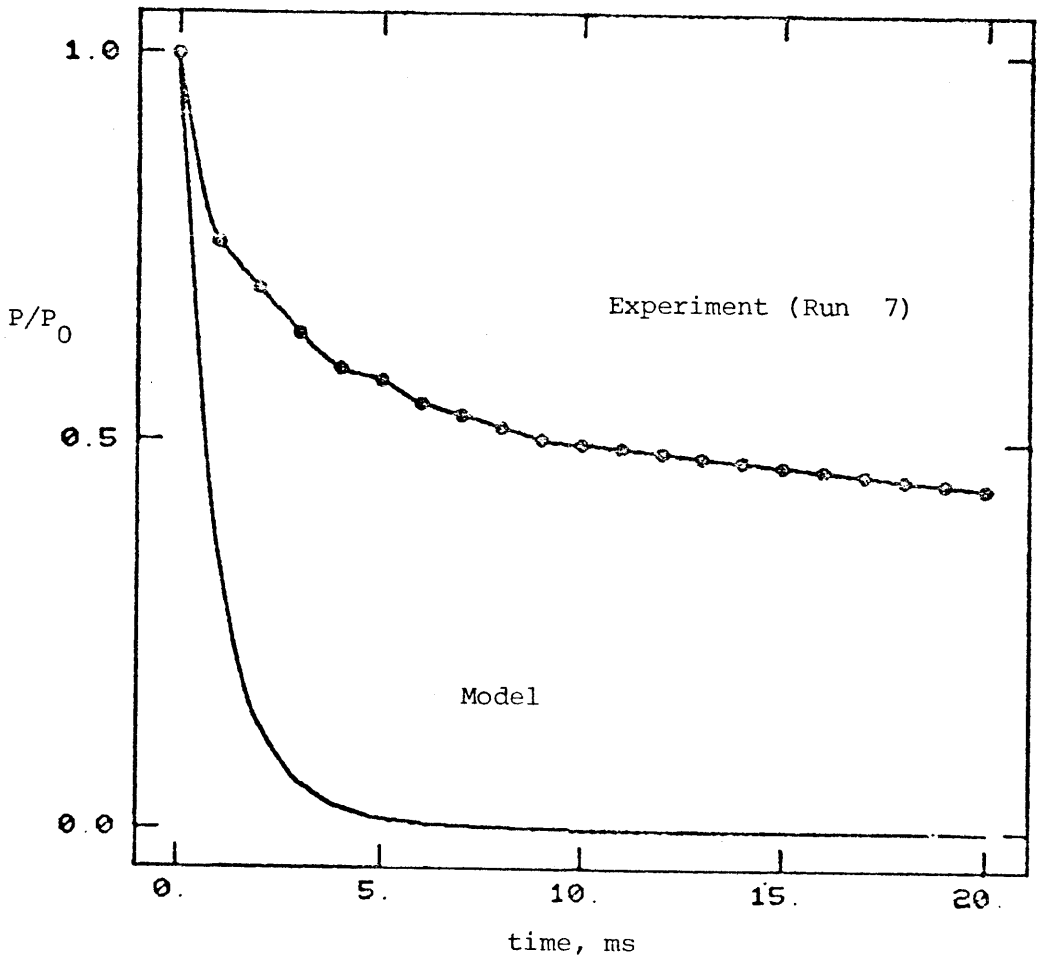

Figure 14a

Comparison of experiment and model predictions for initially saturated CO_2 with P_0=45.8 bar, liquid volume fraction=97.5%. The spinoidal curve for this experiment lies at P/P_0=0.442

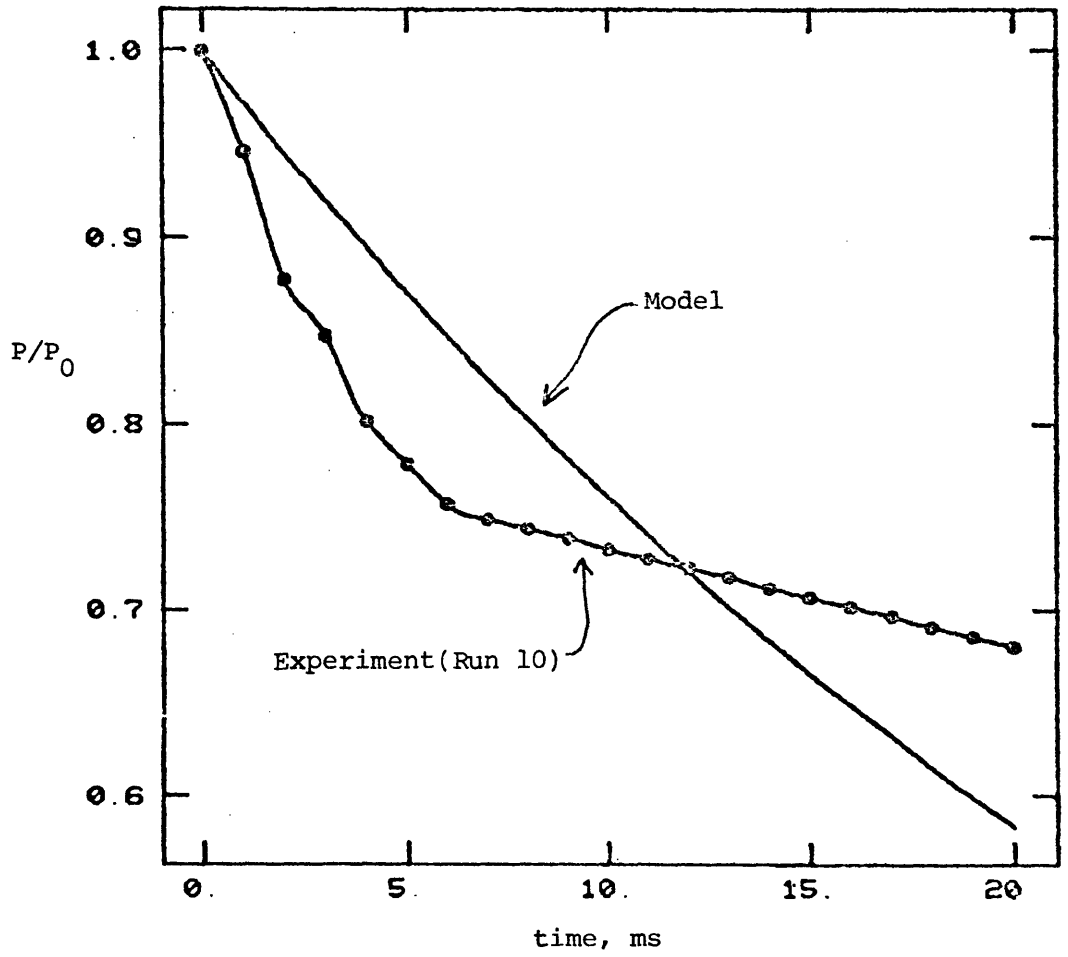

Figure 14b

Comparison of experiment and model predictions for initially supercritical CO_2 with P_0=90.7 bar, V_0=59.02 cm^3/mole. The spinoidal curve for this experiment lies at P/P_0=0.135

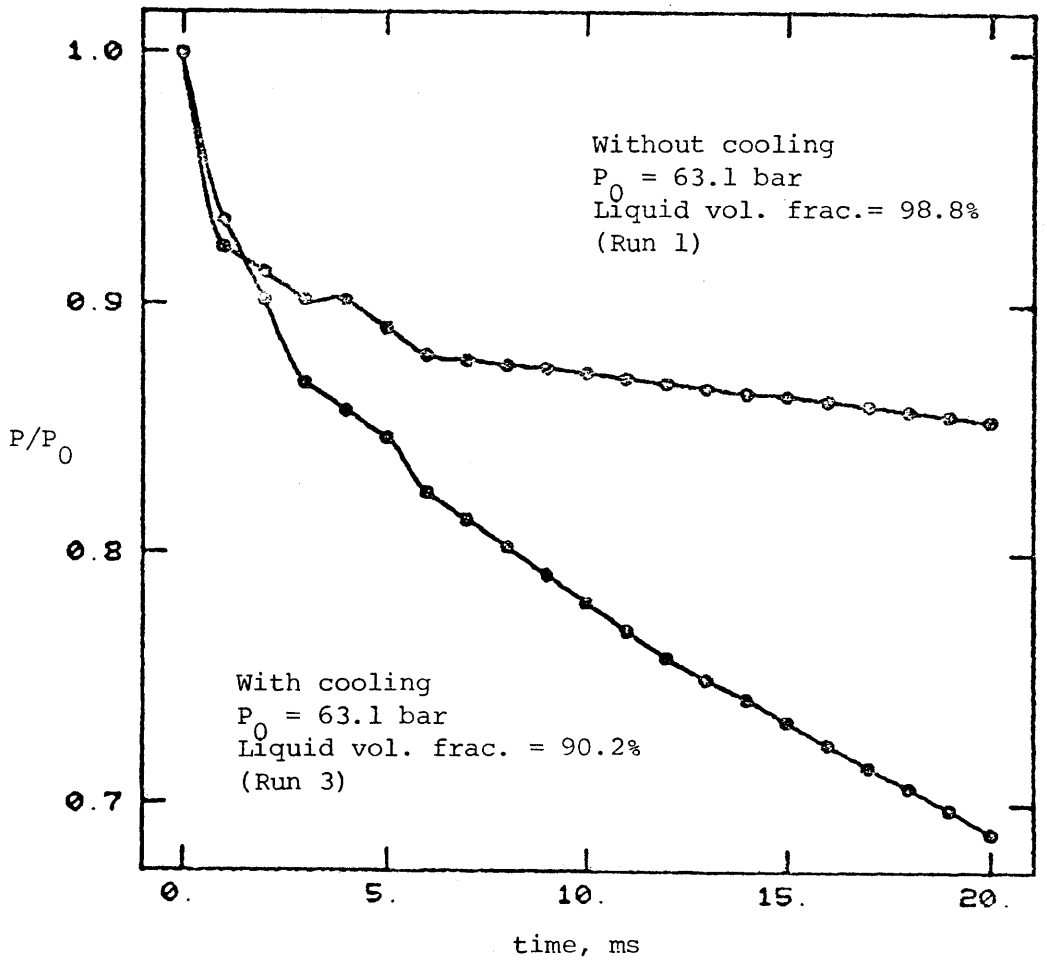

Figure 15a

The effect of wall cooling on a saturated experiment
Spinoidal P/P_0 = 0.627

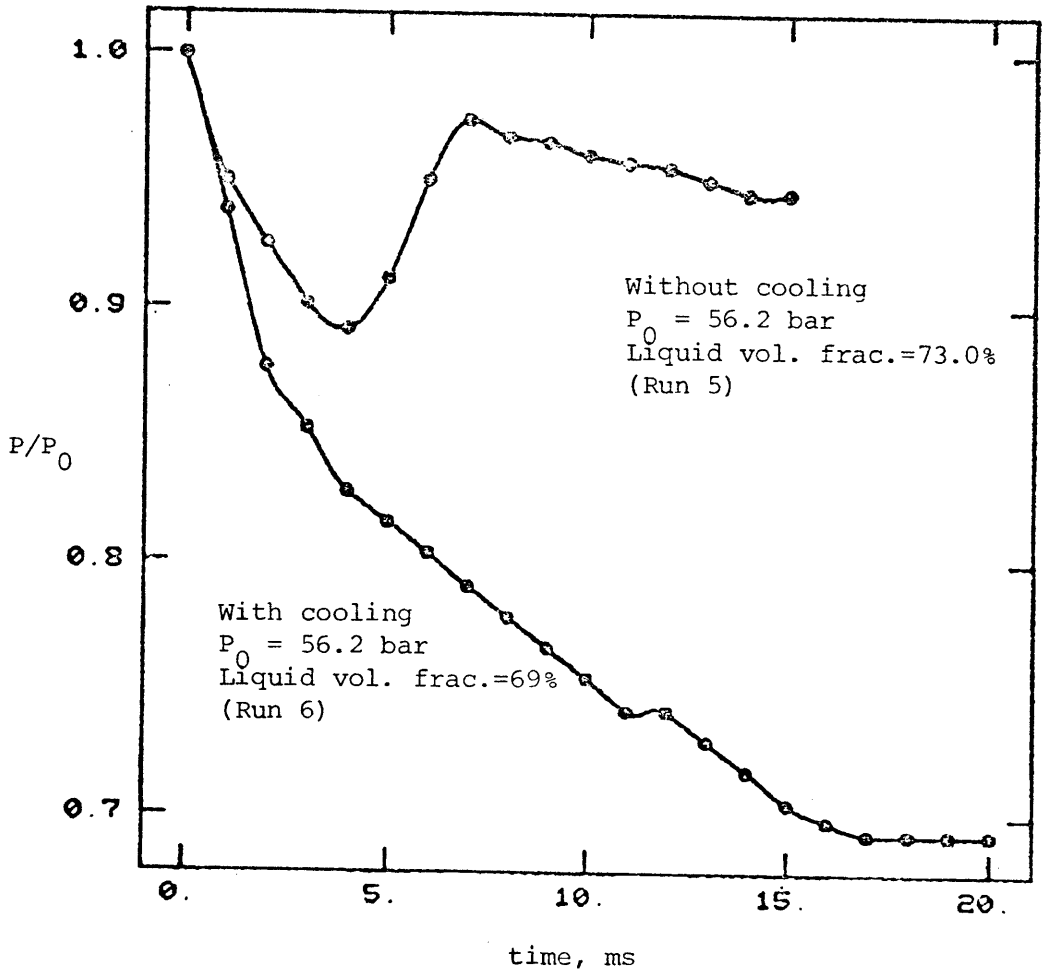

Figure 15b

The effect of wall cooling on a saturated experiment
Spinoidal $P/P_0 = 0.248$

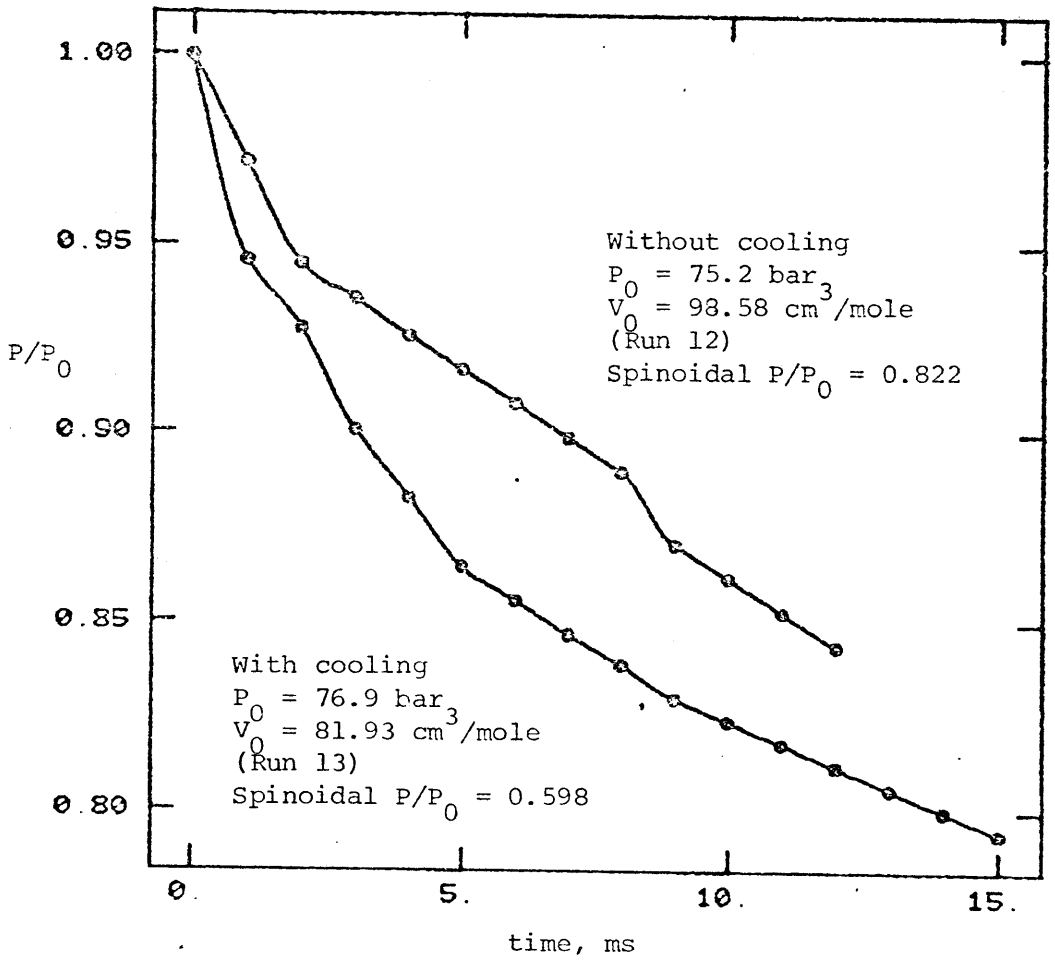

Figure 15c

The effect of wall cooling on a supercritical experiment

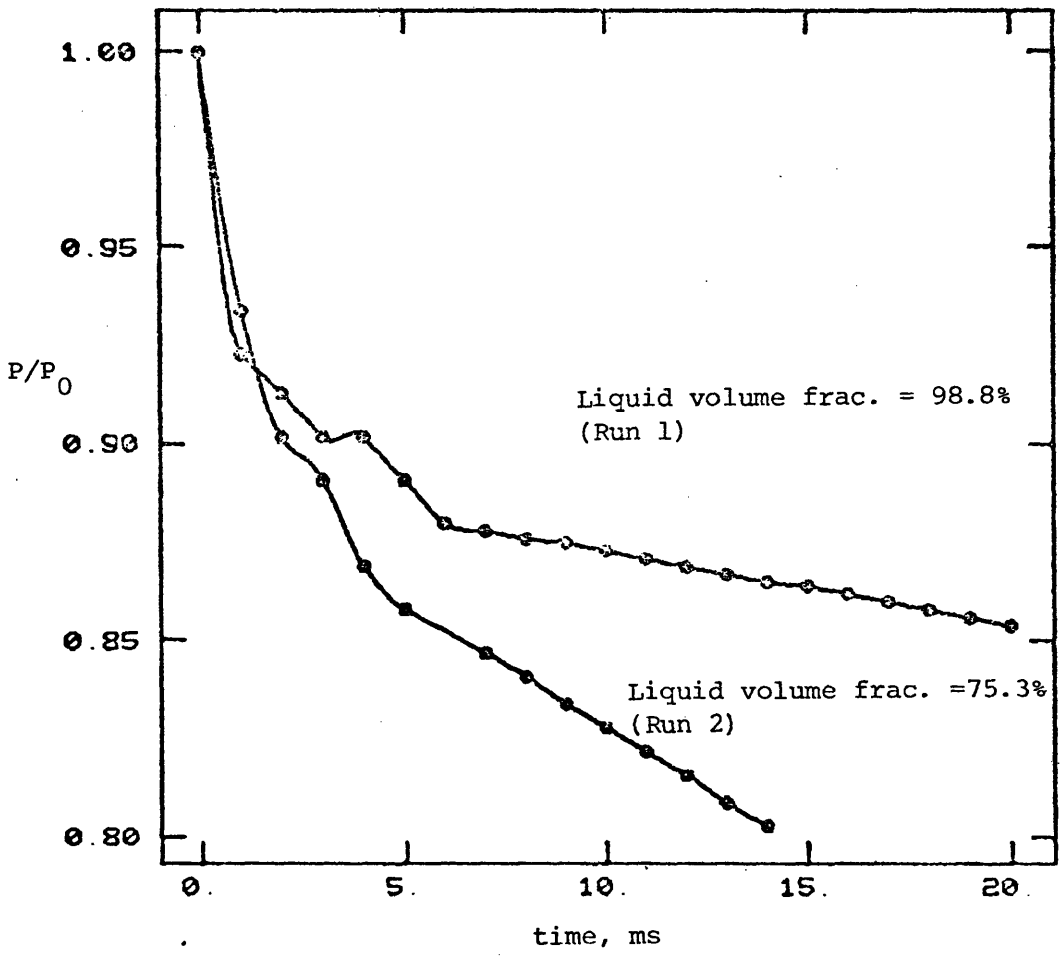

Figure 16a

The effect of liquid level on the depressurization of saturated CO_2
P_0 = 63.1 bar
Spinoidal P/P_0 = 0.627

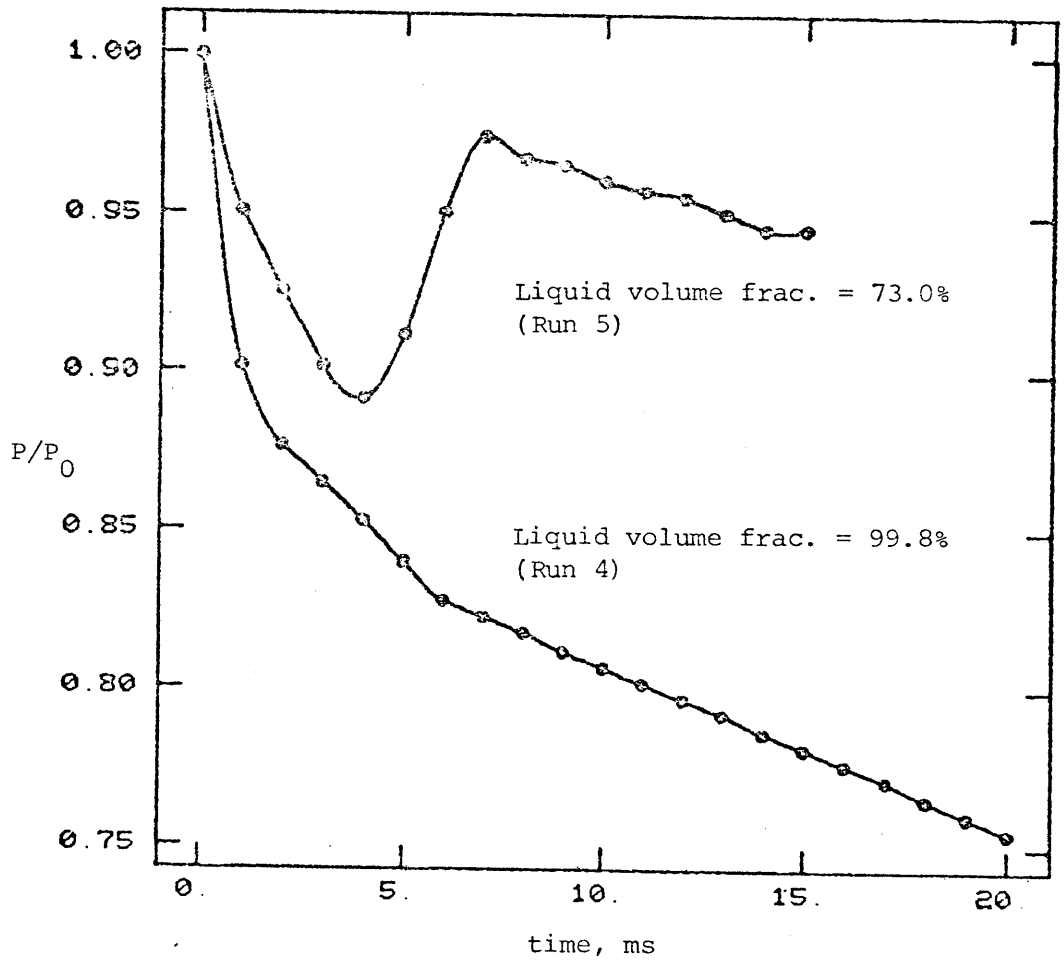

Figure 16b

The effect of liquid level on the depressurization of saturated CO_2
P_0 = 56.2 bar
Spinoidal P/P_0 = 0.248

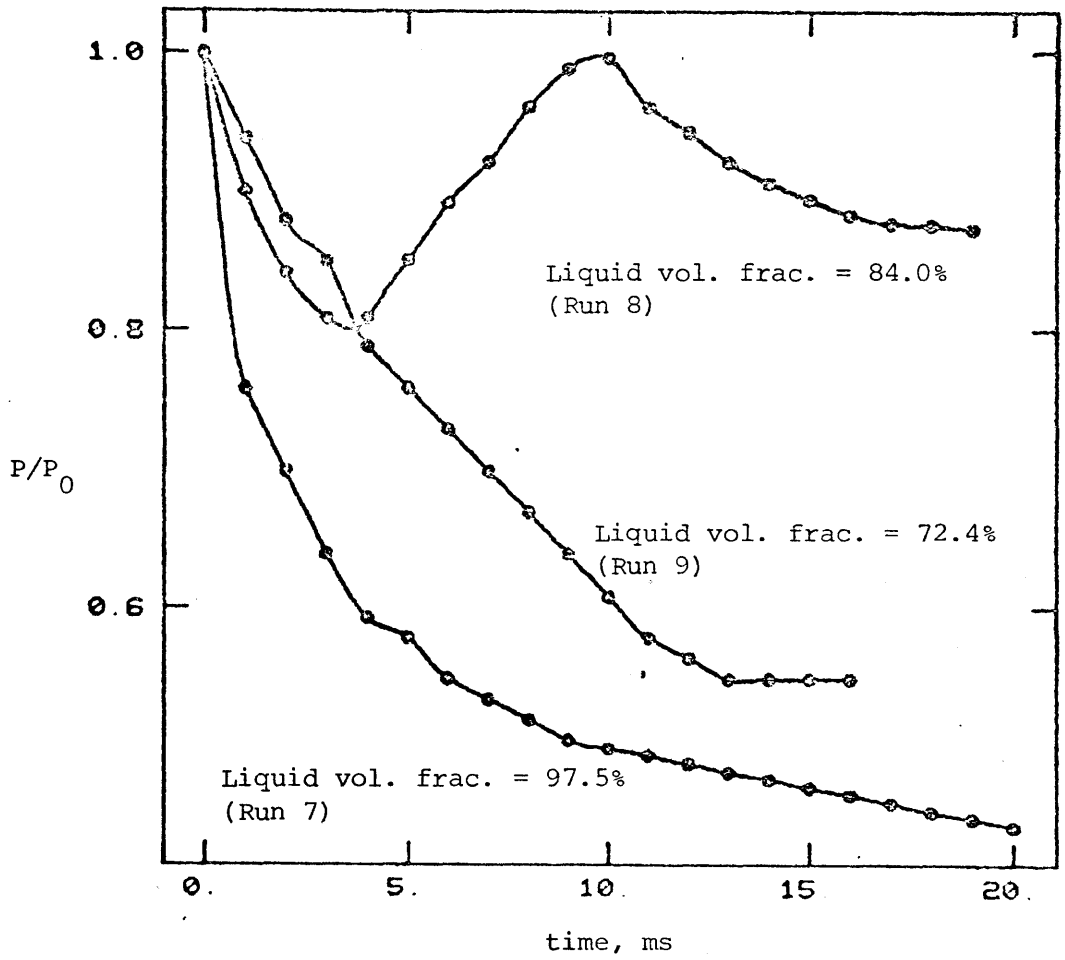

Figure 16c

The effect of liquid level on the depressurization of saturated CO_2
P_0 = 45.8 bar
Spinoidal P/P_0 < 0.0

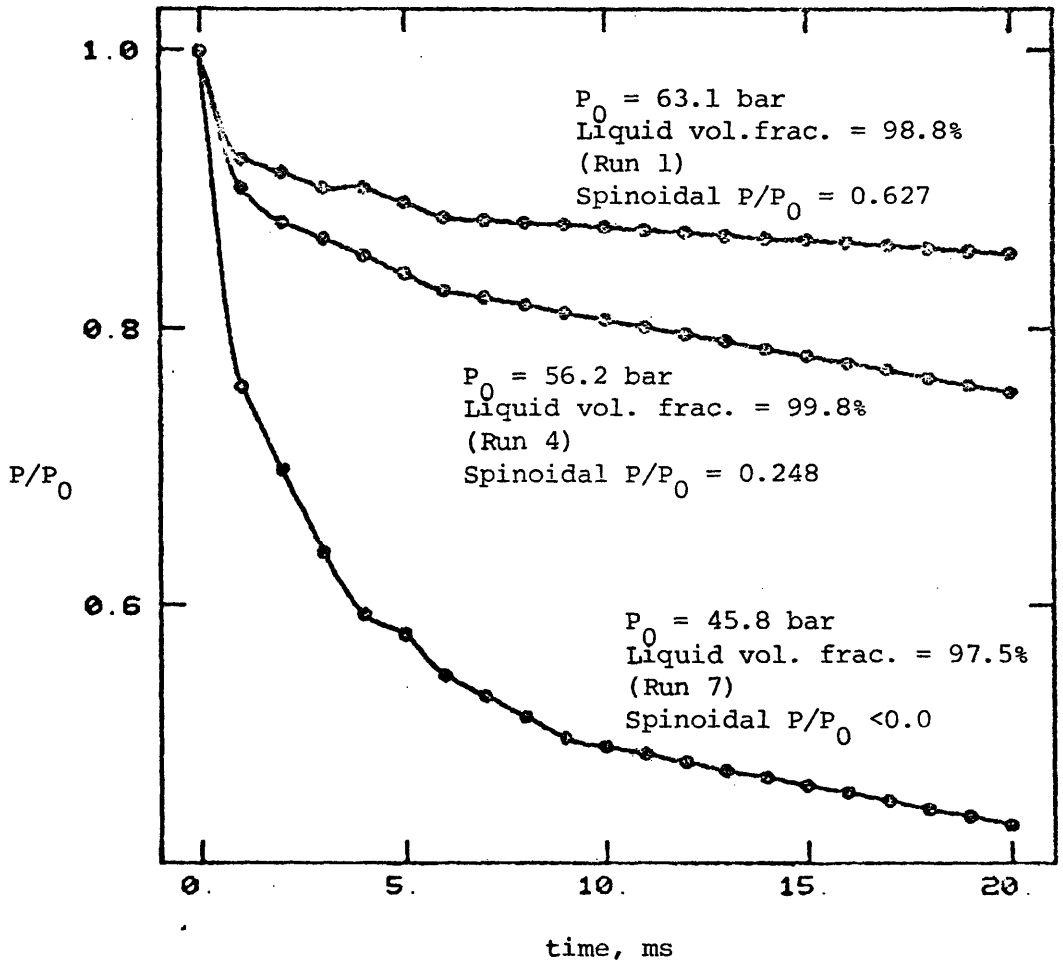

Figure 17a

The effect of initial pressure on the depressurization of saturated CO_2

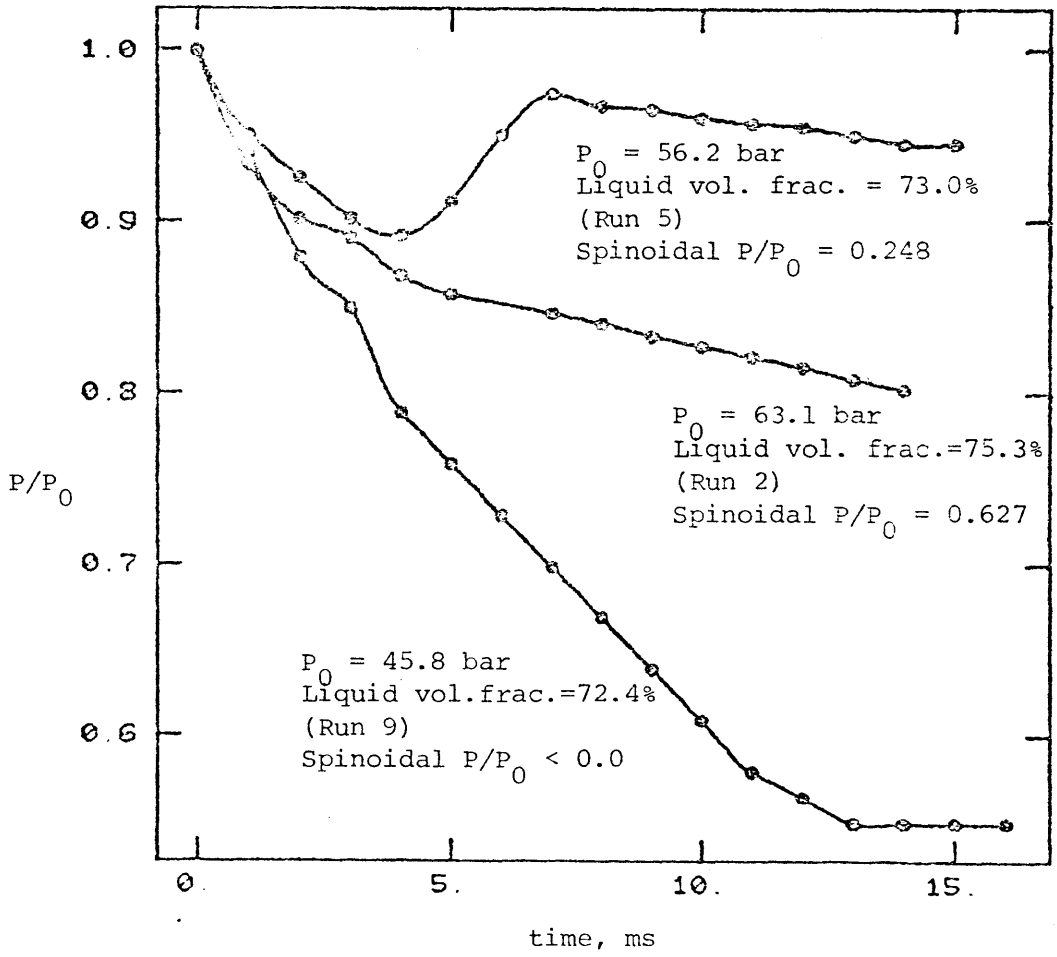

Figure 17b

The effect of initial pressure on the depressurization of saturated CO_2

Table 1

Analysis of a Sample Depressurization

(Initially Saturated CO_2 at 298.4K)

		T, Kelvin			
	(satn.) 298.4	298	296	294	(spin.) 292
P_L, atm	64.0	62.6	56.3	50.1	44.2
P^{sat}, atm (*)	64.0	63.2	60.4	57.7	55.0
V_L, cm^3/mole(**)		70.8	71.6	72.0	74.2
V_v^{sat}, cm^3/mole		182.9	201.1	219.1	237.5
P_v,atm (†)	64.0	63.0	59.0	55.3	51.7
σ, dyne/cm		0.576	0.824	1.09	1.37
$\log_{10}J$	$-\infty$	-173	19.6	24.6	25.0
J	0	0	4.3×10^{19}	4.3×10^{24}	1.0×10^{25}
dP/dT, atm/K			3.17	3.03	2.88
$\frac{d\log_{10}J}{dT} = \frac{2.303}{J}\frac{dJ}{dT}$, K^{-1}			-3.65	-1.35	0.95
r_c, cm		2.8×10^{-6}	6.0×10^{-7}	4.1×10^{-7}	3.6×10^{-7}
V_v, cm^3/mole		193.3	216.4	235.8	303.2
τ_N, sec	∞	∞	7.9×10^{-2}	2.6×10^{-6}	2.1×10^{-6}

(*) superscript "sat" refers to saturation values

(**) V is specific volume

(†) from Blander and Katz, $V_L(P_L-P^{sat}) \simeq P_V V_V \ln(P_V/P^{sat})$

Appendix I
The Peng-Robinson Equation of State

The Peng-Robinson equation of state is:

$$P = \frac{RT}{V-b} - \frac{a(T)}{V(V+b) + b(V-b)} \qquad \text{(I-1)}$$

where P is pressure, R the gas constant, T temperature, V specific volume, and the parameters a and b are given by:

$$a(T) = 0.45724 \frac{R^2 T_c^2}{P_c} \alpha(T_r, \omega)$$

$$b = 0.07780 \frac{RT_c}{P_c}$$

where the subscript "c" denotes its critical value, and the dimensionless function of reduced temperature and acentric factor, $\alpha(T_r, \omega)$, is defined by:

$$\alpha^{1/2} = 1 + \kappa(1 - T_r^{1/2})$$

$$\kappa = 0.37464 + 1.54226\ \omega - 0.26992\ \omega^2$$

Given T and P, V can be calculated by rewriting (I-1) as:

$$Z^3 - (1-B)Z^2 + (A-3B^2-2B)Z - (AB-B^2-B^3) = 0 \qquad \text{(I-2)}$$

where $Z=PV/RT$, $A=aP/R^2T^2$, and $B=bP/RT$.

Physically meaningful roots for (I-2) occur when $Z > B$. In the two-phase region, the largest root is the vapor volume, the smallest positive root is the liquid volume.

The saturation curve can be obtained by equating liquid and vapor fugacities, which can be obtained from:

$$\ln f/P = \int_0^P \left(\frac{V}{RT} - \frac{1}{P}\right) dP$$

which gives:

$$\ln f/P = Z - 1 - \ln(Z-B) - \frac{A}{2.828\ B} \ln\left(\frac{Z+2.414\ B}{Z-0.414\ B}\right) \quad \text{(I-3)}$$

To obtain isentropic paths, the departure function for entropy must be utilized:

$$S(V_2,T) - S(V_1,T) = \int_{V_1}^{V_2} \left(\frac{\partial S}{\partial V}\right)_T dV = \int_{V_1}^{V_2} \left(\frac{\partial P}{\partial T}\right)_V dV$$

Evaluation of the derivative and integral give:

$$S(V_2,T) - S(V_1,T) = R \ln\left[\frac{V_2-b}{V_1-b}\right] + \frac{0.161659 R^2 T_c^{3/2}}{P_c\ b\ T^{1/2}} \kappa \left[1 + \kappa(1-T_r^{1/2})\right] \ln\left[\frac{(V_2-0.4142b)(V_1+2.414b)}{(V_2+2.414\ b)(V_1-0.4142b)}\right]$$

For mixtures, the parameters a and b are functions of the mole fractions, x_i, in the mixture:

$$a = \sum_i \sum_j x_i x_j a_{ij}$$

$$b = \sum_i x_i b_i$$

where $a_{ij} = (1 - \delta_{ij})\ a_i^{1/2}\ a_j^{1/2}$ and δ_{ij} is an empirically determined binary interaction parameter, which can be obtained from data for a binary mixture of components "i" and "j".

Appendix II

A Computer Program for Calculating Isentropic Paths for a Pure Fluid

The program presented here, named "PIZZA", calculates the isentropic path for a pure fluid from its initial state (pressure, P1, temperature, T1) to the spinoidal curve using the Peng-Robinson equation of state. The calculation scheme is illustrated in the following flow chart.

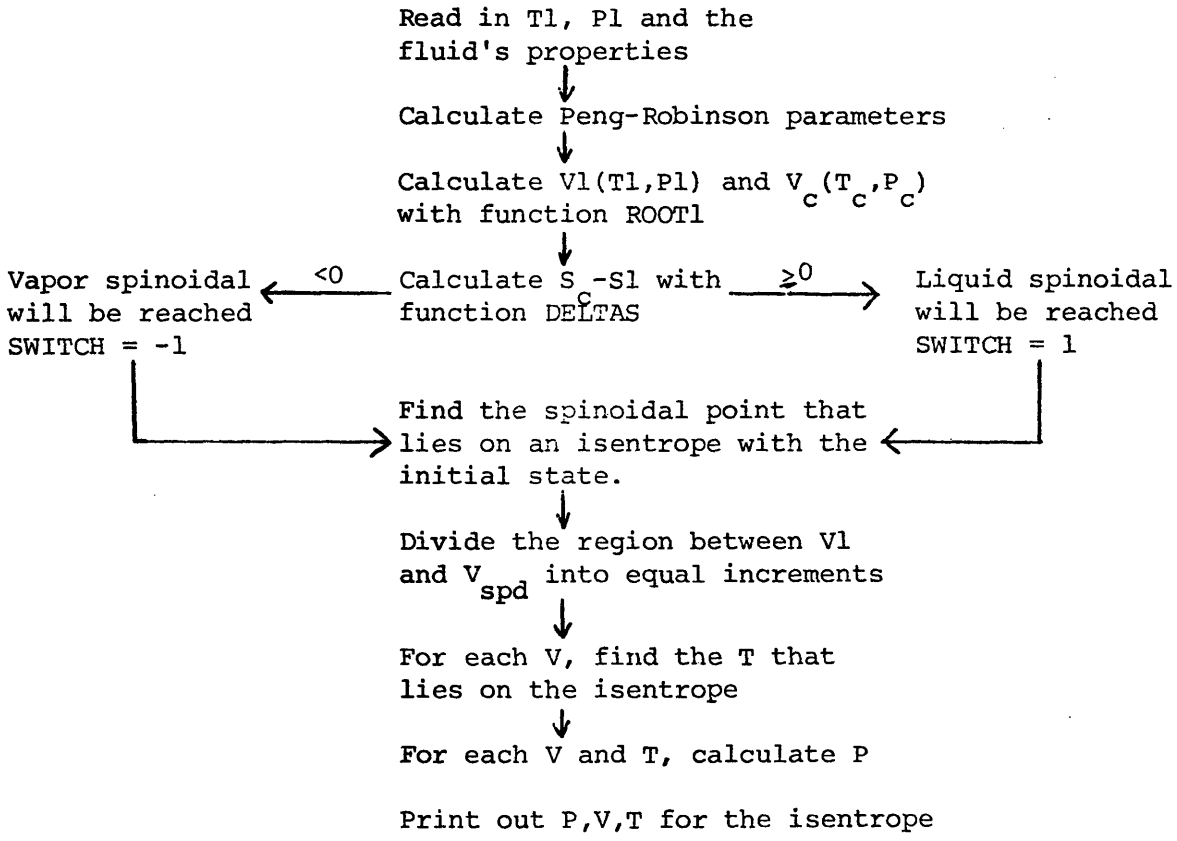

The functions and subroutines used are:

DELTAS(T2,V2,T1,V1,ISKIP).....A function equal to S(T2,V2)-S(T1,V1). Details are given below.

DMAX1(A_1,...,A_n).....An IMSL function that determines the maximum value among the A's.

DMIN1(A_1,...,A_n).....An IMSL function that determines the minimum value among the A's.

ENTRO1(T,V2,V1) .....A function equal to S(T,V2)-S(T,V1).

ROOT1(T,P).....A function equal to V, given a T and P in the single-phase region.

SATN(T,VL,VV,P).....Given T, this subroutine calculates the pressure (P), liquid volume (VL), and vapor volume (VV), on the saturation curve by matching fugacities.

ZPOLR(A,N,Z,IER).....An IMSL subroutine that finds the (complex) roots, Z, for the N-th order polynomial:

$$\sum_{j=1}^{N} A_j Z^{N-j} = 0$$

When applicable, the Peng-Robinson equation was used. The function DELTAS is used to generate the isentropic path by guessing T2 (given V2,T1, and V1), and improving this guess until DELTAS becomes less than some acceptable value. Since the departure functions developed in Appendix I involve isotherms, the temperature change must be incorporated in some way. For a pure fluid, the most straightforward manner is to rewrite the entropy difference as:

$$S(T2,V2) - S(T1,V1) = [S(T2,V2)-S(T2,V_L^{sat})]^* + [S(T2,V_L^{sat})-S(T2,V_V^{sat})]^\dagger + [S(T2,V_V^{sat})-S(T2,V_\infty)]^* + [S(T2,V_\infty)-S(T1,V_\infty)] + [S(T1,V_\infty)-S(T1,V_V^{sat})]^* + [S(T1,V_V^{sat})-S(T1,V_L^{sat})]^\dagger + [S(T1,V_L^{sat})-S(T1,V1)]^* \quad \text{(II-1)}$$

where the subscripts "L" and "V" refer to the liquid and vapor phases, respectively, and "sat" refers to the saturation curve.

The differences marked by an asterisk can be evaluated using the departure function for entropy. The differences marked by a cross are equal to entropies of vaporization; these can be evaluated by using the Clausius-Clapeyron equation:

$$\Delta S^{vap} = \frac{\Delta H^{vap}}{T} = \frac{-R \ \Delta Z^{vap}}{T} \ \frac{d \ln P^{sat}}{d(1/T)} \quad \text{(II-2)}$$

The difference at V_∞ can be evaluated using the ideal gas heat capacities provided that V_∞ is chosen such that the fluid is truly an ideal gas in that temperature range. The ideal gas heat capacity can be expressed as:

$$C_V^* = a + bT + cT^2 + dT^3 - R \quad \text{(II-3)}$$

Values for the coefficients for a wide variety of compounds are given in Reid, Prausnitz, and Sherwood (1977).

The derivative in the Clausius-Clapeyron equation was evaluated by using finite differences; saturation properties were calculated at temperature T and T+ΔT. For ΔT = 1 K, values for the entropy of vaporization obtained in this manner were always within 5% of values reported by IUPAC (Angus et al. 1973).

Since PIZZA always calculates entropy differences between a guessed

state and the initial state, the last three terms in (II-1) that just involve T1 need only be calculated the first time DELTAS is used. So, DELTAS will calculate all of the terms in (II-1) if the parameter ISKIP = 0. If ISKIP $\neq$ 0, the calculations involving T1 will not be repeated.

In order to find temperatures on the isentrope, an initial guess is made and improvements to this guess are made by an Euler-like method:

$$T^{(k)} = T^{(k-1)} - \varepsilon[S(T^{(k-1)},V)-S(T1,V1)] \qquad \text{(II-4)}$$

where ε is a positive constant.

At present, the program is too time-consuming due to its generality. For each temperature guess, SATN will be run to get saturation properties. Since SATN also uses an iterative procedure, a large number of calculations result to find just one point on the isentrope. Modifications can be made to improve convergence, the most helpful ones being:

(a) Before running PIZZA, run SATN for a wide range of temperatures, then empirically determine $P^{sat}(T)$, $V_L^{sat}(T)$ and $V_v^{sat}(T)$ as functions that are polynomials in T using a normal regression analysis. This will eliminate the need for SATN when running PIZZA. Also, P^{sat} can then be differentiated and plugged into (II-2) to give an analytic expression for ΔS^{vap}.

(b) Use a better method for finding the temperatures on an isentrope. With (II-4), it is possible for the search to oscillate about, without converging to, the correct T. However, if ε is initially large, then gradually reduced as the correct T is approached, then this instability can be eliminated and convergence will be fairly rapid. A Newton-Raphson method would converge faster:

$$T^{(k)} = T^{(k-1)} - \frac{[S(T^{(k-1)},V) - S(T1,V1)]}{\left[\frac{\partial S(T,V)}{\partial T}\right]_{T=T^{(k-1)}}}$$

However, convergence of the Newton-Raphson method is very sensitive to the initial guess. This may make the Euler-like method better suited for use in PIZZA.

The following are key terms in PIZZA and its subroutines.

A,B,Al,CAP - parameters of the Peng-Robinson equation of state

ALIMIT - if |DELTAS| < ALIMIT, convergence is obtained

CPA,CPB,CPC,CPD - coefficients in (II-3)

DT - ΔT for evaluating (II-2) by finite differences

EPS - ϵ in (II-4)

FUGL,FUGV - expressions for the fugacity of liquid and vapor phases from (I-3)

IDELT,IPIZZ,ISATN - debugging aids; if non-zero, these will print values for variables in various parts of the program. If equal to zero, this printing is suppressed.

IMAX - maximum number of iterations permitted

ISKIP - a parameter in DELTAS, which was explained in the discussion of DELTAS

ITER,JIT - iteration number

NN - number of intervals in volume desired between the initial and spinoidal states

PENG(J),SAT(J) - coefficients from (I-2) for use in ZPOLR

PC,TC,VC - critical pressure, temperature, and volume

PRAY(J),VRAY(J),TRAY(J) - pressure, volume, temperature on the isentrope

Pl,Vl,Tl - initial pressure, volume, temperature

R,RJPG - gas constant with units bar-cm^3/mol-K and joule/mol-K

SPIN(J) - coefficients from (5) for use in ZPOLR

SWITCH - if the liquid spinoidal will be reached, SWITCH = 1
if the vapor spinoidal will be reached, SWITCH = -1

TSPD, VSPD - spinoidal temperature and volume

VINF - V_∞ in (II-1)

W - acentric factor

```
FILE: PIZZA     FORTRAN  A                    CONVERSATIONAL MONITOR SYSTEM

      IMPLICIT REAL*8(A-H,O-Z)                                                  PIZ00010
      INTEGER SWITCH                                                            PIZ00020
      COMPLEX*16 Z(4)                                                           PIZ00030
      DIMENSION SPIN(5),VRAY(100),TRAY(100),PRAY(100),VR(4),VI(4)               PIZ00040
      COMMON/ONE/R,RJPG,A1,B,CAP,TC,PC,W                                        PIZ00050
      COMMON/TWO/VINF,DT,CPA,CPB,CPC,CPD                                        PIZ00060
      COMMON/THR/VL1,VV1,PSAT1,DZVAP1,DSVAP1,VL2,VV2,PSAT2,DZVAP2,DSVAP2PIZ00070
      COMMON/FOR/IDELT,IPIZZ,ISATN                                              PIZ00080
      R=83.14                                                                   PIZ00090
      RJPG=8.314                                                                PIZ00100
C*****READ IN TC,PC,W,INITIAL T AND P, V-INFINITY AND                           PIZ00110
C*****CPA,...,CPD WHERE CP*=CPA+CPB*T+CPC*T**2+CPD*T**3                         PIZ00120
      READ(5,*)TC,PC,W,VINF                                                     PIZ00130
      READ(5,*)T1,P1,CPA,CPB,CPC,CPD                                            PIZ00140
      READ(5,*) DT,IMAX,EPS,ALIMIT,NN                                           PIZ00150
      READ(5,*)IPIZZ,ISATN,IDELT                                                PIZ00160
      WRITE(6,1000)TC,PC,W,VINF                                                 PIZ00170
      WRITE(6,1010)T1,P1,CPA,CPB,CPC,CPD                                        PIZ00180
      WRITE(6,1015)DT,IMAX,EPS,ALIMIT,NN                                        PIZ00190
C*****GET PENG-ROB PARAMETERS                                                   PIZ00200
      B=0.07780*R*TC/PC                                                         PIZ00210
      A1=0.45724*(R*TC)**2/PC                                                   PIZ00220
      CAP=0.37464+ 1.54226*W - 0.26992*W*W                                      PIZ00230
C*****CALCULATE VINIT AND SATN. VOLS. AND ENTROPY OF VAP. AT T1                 PIZ00240
      V1=ROOT1(T1,P1)                                                           PIZ00250
      VC=ROOT1(TC,PC)                                                           PIZ00260
      DSCRIT=DELTAS(TC,VC,T1,V1,0)                                              PIZ00270
      IF(IPIZZ.EQ.0) GO TO 12                                                   PIZ00280
      WRITE(6,2)DSCRIT                                                          PIZ00290
2     FORMAT('DSCRIT=',D15.5)                                                   PIZ00300
12    CONTINUE                                                                  PIZ00310
      IF(DSCRIT.GE.0.) SWITCH=1                                                 PIZ00320
      IF(DSCRIT.LT.0.) SWITCH=-1                                                PIZ00330
C**  SWITCH=1 (LIQUID SPIN)     SWITCH=-1 (VAPOR SPIN)                         PIZ00340
C**** FIND SPIN POINT                                                           PIZ00350
      TSPD=DMIN1(T1,TC)                                                         PIZ00360
      ITER=0                                                                    PIZ00370
50    IF(ITER.GE.IMAX) GO TO 925                                                PIZ00380
      A=A1*(1.+CAP*(1.-DSQRT(TSPD/TC)))**2                                      PIZ00390
      CALL SATN(TSPD,VL,VV,P)                                                   PIZ00400
      VL2=VL                                                                    PIZ00410
      VV2=VV                                                                    PIZ00420
      PSAT2=P                                                                   PIZ00430
      IF(IPIZZ.EQ.0) GO TO 13                                                   PIZ00440
      WRITE(6,1)VL2,VV2,PSAT2                                                   PIZ00450
1     FORMAT('******',3F10.5,'*********')                                       PIZ00460
13    CONTINUE                                                                  PIZ00470
      IF(TSPD.EQ.TC)VSPD=VL2                                                    PIZ00480
      IF(TSPD.EQ.TC) GO TO 55                                                   PIZ00490
      IF(IPIZZ.EQ.0) GO TO 14                                                   PIZ00500
      WRITE(6,67) VSPD                                                          PIZ00510
67    FORMAT('VSPD=  ',D15.5)                                                   PIZ00520
14    CONTINUE                                                                  PIZ00530
      CON=A/R/TSPD                                                              PIZ00540
      SPIN(1)=1.D0                                                              PIZ00550
```

```
      SPIN(2)=4.*B-2.*CON                                              PIZ00560
      SPIN(3)=2.*B*(B+CON)                                             PIZ00570
      SPIN(4)=2.*B*B*(CON-2.*B)                                        PIZ00580
      SPIN(5)=(B-2.*CON)*B*B*B                                         PIZ00590
      CALL ZPOLR(SPIN,4,Z,IER)                                         PIZ00600
      IF(SWITCH.EQ.-1) GO TO 40                                        PIZ00610
      DO 35 J=1,4                                                      PIZ00620
      VR(J)=REAL(Z(J))                                                 PIZ00630
      VI(J)=AIMAG(Z(J))                                                PIZ00640
      IF(VI(J).NE.0.0) VR(J)=1.D20                                     PIZ00650
      IF(VR(J).LE.VL2) VR(J)=1.D25                                     PIZ00660
      IF(IPIZZ.EQ.0) GO TO 15                                          PIZ00670
      WRITE(6,3)SWITCH,VR(J),TSPD                                      PIZ00680
3     FORMAT('SWITCH =  ',I2,5X,D15.5,5X,F10.5)                        PIZ00690
15    CONTINUE                                                         PIZ00700
35     CONTINUE                                                        PIZ00710
      VSPD=DMIN1(VR(1),VR(2),VR(3),VR(4))                              PIZ00720
      GO TO 55                                                         PIZ00730
40    DO 45 J=1,4                                                      PIZ00740
      VR(J)=REAL(Z(J))                                                 PIZ00750
      VI(J)=AIMAG(Z(J))                                                PIZ00760
      IF(VI(J).NE.0.0) VR(J)=-1.D20                                    PIZ00770
      IF(VR(J).GE.VV2) VR(J)=-1.D25                                    PIZ00780
      IF(IPIZZ.EQ.0) GO TO 45                                          PIZ00790
      WRITE(6,3)SWITCH,VR(J),TSPD                                      PIZ00800
45    CONTINUE                                                         PIZ00810
      VSPD=DMAX1(VR(1),VR(2),VR(3),VR(4))                              PIZ00820
55    DSPDS=DELTAS(TSPD,VSPD,T1,V1,1)                                  PIZ00830
      IF(DABS(DSPDS).LE.ALIMIT) GO TO 100                              PIZ00840
      IF(DSPDS.LT.0.0) GO TO 60                                        PIZ00850
      TSPD=TSPD-EPS*SWITCH*DABS(DSPDS)                                 PIZ00860
      IF(IPIZZ.EQ.0) GO TO 16                                          PIZ00870
      WRITE(6,89)ITER,SWITCH,TSPD                                      PIZ00880
89    FORMAT('ITER= ',I4,5X,'SWITCH =  ',I3, 5X,F10.5)                 PIZ00890
16    CONTINUE                                                         PIZ00900
      ITER=ITER+1                                                      PIZ00910
      GO TO 50                                                         PIZ00920
60    TSPD=TSPD+EPS*SWITCH*DABS(DSPDS)                                 PIZ00930
      IF(IPIZZ.EQ.0) GO TO 17                                          PIZ00940
      WRITE(6,89)ITER,SWITCH,TSPD                                      PIZ00950
17    CONTINUE                                                         PIZ00960
      ITER=ITER+1                                                      PIZ00970
      GO TO 50                                                         PIZ00980
C**NOW GENERATE THE TRAJECTORY                                         PIZ00990
C                                                                      PIZ01000
100   CONTINUE                                                         PIZ01010
      IF(SWITCH.EQ.1)WRITE(6,1030)                                     PIZ01020
      IF(SWITCH.EQ.-1) WRITE(6,1040)                                   PIZ01030
      WRITE(6,1060)                                                    PIZ01040
      DO 200 J=1,NN                                                    PIZ01050
      JIT=0                                                            PIZ01060
      VRAY(J)=V1 +(VSPD-V1)*J/NN                                       PIZ01070
      IF(J.EQ.1) TRAY(J)=T1                                            PIZ01080
      IF(J.EQ.1) GO TO 110                                             PIZ01090
      TRAY(J)=TRAY(J-1)                                                PIZ01100
```

```
      TRAY(NN)=TSPD                                                    PIZ01110
110   IF(JIT.GE.IMAX) GO TO 930                                        PIZ01120
      DSRAY=DELTAS(TRAY(J),VRAY(J),T1,V1,1)                            PIZ01130
      IF(DABS(DSRAY).LE.ALIMIT) GO TO 180                              PIZ01140
      IF(DSRAY.LT.0.) GO TO 120                                        PIZ01150
      TRAY(J)=TRAY(J)-EPS*DABS(DSRAY)                                  PIZ01160
      JIT=JIT+1                                                        PIZ01170
      GO TO 110                                                        PIZ01180
120   TRAY(J)=TRAY(J)+EPS*DABS(DSRAY)                                  PIZ01190
      JIT=JIT+1                                                        PIZ01200
      GO TO 110                                                        PIZ01210
180   A=A1*(1.+CAP*(1.-DSQRT(TRAY(J)/TC)))**2                          PIZ01220
      PRAY(J)=R*TRAY(J)/(VRAY(J)-B) -A/(VRAY(J)*VRAY(J)+2.*VRAY(J)     PIZ01230
     **B-B*B)                                                          PIZ01240
      WRITE(6,1070) TRAY(J),PRAY(J),VRAY(J)                            PIZ01250
200   CONTINUE                                                         PIZ01260
      GO TO 999                                                        PIZ01270
925   WRITE(6,1080)IMAX,TSPD                                           PIZ01280
      GO TO 999                                                        PIZ01290
930   WRITE(6,1090)IMAX,J,TRAY(J)                                      PIZ01300
C                                                                      PIZ01310
1000  FORMAT('TC=',F10.5,2X,'PC=',F10.5,2X,'W=',F10.5,2X,'VINF=',D15.5) PIZ01320
1010  FORMAT('T1=',F10.5,2X,'P1=',F10.5,/,'CPA,B,C,D = ',4D15.5)       PIZ01330
1015  FORMAT('DT= ',F10.5,5X,'IMAX= ',I5,5X,'EPS= ',D15.5,/            PIZ01340
     *,'ALIMIT= ',D15.5,5X,'NN =',I3)                                  PIZ01350
1030  FORMAT(' THE LIQUID SPINOIDAL CURVE WILL BE APPROACHED')         PIZ01360
1040  FORMAT(' THE VAPOR SPINOIDAL CURVE WILL BE APPROACHED')          PIZ01370
1060  FORMAT(/,' THE ISENTROPIC PATH IS AS FOLLOWS:',//,               PIZ01380
     *'TEMPERATURE,KELVIN',10X,'PRESSURE,BARS',10X,'VOLUME,CC/MOL',/)  PIZ01390
1070  FORMAT(4X,F10.3,15X,F10.3,13X,F10.3)                             PIZ01400
1080  FORMAT(I10,' ITERATIONS EXCEEDED FROMTHE SPINOIDAL CALC. AT      PIZ01410
     *   ',F10.3,'  KELVIN')                                           PIZ01420
1090  FORMAT(I10,' ITERATIONS EXCEEDED ON DATA PT. NO. ',I3,'          PIZ01430
     *  AT   ',F10.3,'  KELVIN')                                       PIZ01440
C                                                                      PIZ01450
999   STOP                                                             PIZ01460
      END                                                              PIZ01470
```

```
FILE: ENTRO1    FORTRAN  A                    CONVERSATIONAL MONITOR SYSTEM

      FUNCTION ENTRO1(T,V2,V1)                                         ENT00010
C                                                                      ENT00020
C   ENTROPY DEPARTURE FUNCTION - - PENG-ROBINSON EQ. OF STATE          ENT00030
C                                                                      ENT00040
C   ENTRO(T,V2,V1) = S(T,V2) - S(T,V1)                                 ENT00050
C                                                                      ENT00060
      IMPLICIT REAL*8(A-H,O-Z)                                         ENT00070
      COMMON/ONE/R,RUPG,A1,B,CAP,TC,PC,W                               ENT00080
      SPAR1=DLOG((V2-B)/(V1-B))                                        ENT00090
      A2=1.+CAP*(1.-DSQRT(T/TC))                                       ENT00100
      SPAR2=.161659*A2*R*TC**1.5*CAP/PC/DSQRT(T)/B                     ENT00110
      SPAR2=SPAR2*DLOG((V2-.414214*B)*(V1+2.414214*B)/(V2+2.414214     ENT00120
     1*B)/(V1-.414214*B))                                              ENT00130
      ENTRO1=RUPG*(SPAR1+SPAR2)                                        ENT00140
      RETURN                                                           ENT00150
      END                                                              ENT00160
```

FILE: DELTAS FORTRAN A CONVERSATIONAL MONITOR SYSTEM

```
      FUNCTION DELTAS(T2,V2,T1,V1,ISKIP)                                DEL00010
      IMPLICIT REAL*8(A-H,O-Z)                                          DEL00020
      INTEGER IDELT                                                     DEL00030
      COMMON/ONE/R,RJPG,A1,B,CAP,TC,PC,W                                DEL00040
      COMMON/TWO/VINF,DT,CPA,CPB,CPC,CPD                                DEL00050
      COMMON/THR/VL1,VV1,PSAT1,DZVAP1,DSVAP1,VL2,VV2,PSAT2,DZVAP2,DSVAP2DEL00060
      COMMON/FOR/IDELT,IPIZZ,ISATN                                      DEL00070
      IF(ISKIP.NE.0)GO TO 20                                            DEL00080
C** CALC PARTS A,B,C                                                    DEL00090
      IF(T1.GE.TC) GO TO 10                                             DEL00100
      CALL SATN(T1,VL1,VV1,PSAT1)                                       DEL00110
      DZVAP1=(VV1-VL1)*PSAT1/R/T1                                       DEL00120
      TNEXT=T1+DT                                                       DEL00130
      IF(TNEXT.GT.TC) TNEXT=TC                                          DEL00140
      CALL SATN(TNEXT,VL,VV,PNEXT)                                      DEL00150
      DSVAP1=DZVAP1*DLOG(PNEXT/PSAT1)/(-1./TNEXT + 1./T1)*RJPG/T1       DEL00160
      PARTA=ENTRO1(T1,VL1,V1)                                           DEL00170
      PARTB=DSVAP1                                                      DEL00180
      PARTC=ENTRO1(T1,VINF,VV1)                                         DEL00190
      GO TO 20                                                          DEL00200
10    PARTA=ENTRO1(T1,VINF,V1)                                          DEL00210
      PARTB=0.0                                                         DEL00220
      PARTC=0.0                                                         DEL00230
20    CONTINUE                                                          DEL00240
C** CALC PARTS D THRU G                                                 DEL00250
      PARTD=(CPA-1.987)*DLOG(T2/T1)+ CPB*(T2-T1)+ CPC*(T2*T2-T1*T1)     DEL00260
     */2.  + CPD*(T2**3-T1**3)/3.                                       DEL00270
      PARTD=PARTD*4.1868                                                DEL00280
      IF(T2.GE.TC) GO TO 50                                             DEL00290
      VC=ROOT1(TC,PC)                                                   DEL00300
      IF(V2.GE.VC) GO TO 50                                             DEL00310
      CALL SATN(T2,VL2,VV2,PSAT2)                                       DEL00320
      DZVAP2=(VV2-VL2)*PSAT2/R/T2                                       DEL00330
      TNEXT=T2+DT                                                       DEL00340
      IF(TNEXT.GT.TC) TNEXT=TC                                          DEL00350
      CALL SATN(TNEXT,VL,VV,PNEXT)                                      DEL00360
      DSVAP2=DZVAP2*DLOG(PNEXT/PSAT2)/(-1./TNEXT +1./T2)*RJPG/T2        DEL00370
      PARTE=ENTRO1(T2,VV2,VINF)                                         DEL00380
      PARTF=(-1.)*DSVAP2                                                DEL00390
      PARTG=ENTRO1(T2,V2,VL2)                                           DEL00400
      GO TO 60                                                          DEL00410
50    PARTE=ENTRO1(T2,V2,VINF)                                          DEL00420
      PARTF=0.0                                                         DEL00430
      PARTG=0.0                                                         DEL00440
60    DELTAS=PARTA+PARTB+PARTC+PARTD+PARTE+PARTF+PARTG                  DEL00450
      IF(IDELT.EQ.0) GO TO 65                                           DEL00460
      WRITE(6,1)                                                        DEL00470
1     FORMAT('FROM DELTAS:')                                            DEL00480
      WRITE(6,5)T2,V2,T1,V1                                             DEL00490
      WRITE(6,6)VL1,VV1,PSAT1                                           DEL00500
      WRITE(6,6)VL2,VV2,PSAT2                                           DEL00510
6     FORMAT(3D15.5)                                                    DEL00520
      WRITE(6,4)PARTA,PARTB,PARTC                                       DEL00530
      WRITE(6,5)PARTD,PARTE,PARTF,PARTG                                 DEL00540
      WRITE(6,7)DELTAS                                                  DEL00550

4     FORMAT(3D15.5)                                                    DEL00560
5     FORMAT(4D15.5)                                                    DEL00570
7     FORMAT('DELTAS =  ',D15.5)                                        DEL00580
65    CONTINUE                                                          DEL00590
      RETURN                                                            DEL00600
      END                                                               DEL00610
```

```
FILE: SATN     FORTRAN  A                    CONVERSATIONAL MONITOR SYSTEM

      SUBROUTINE SATN(T,VLSAT,VVSAT,P)                                  SAT00010
C                                                                       SAT00020
C  GIVEN A T (KELVIN),  SATN GIVES SATURATION LIQUID                    SAT00030
C  AND VAPOR VOLUMES (CC/MOL) AND THE SATURATION PRESSURE (BARS)        SAT00040
C  BY EQUATING FUGACITIES CALCULATED WITH THE PENG-ROBINSON EQ. OF STATESAT00050
C                                                                       SAT00060
      IMPLICIT REAL *8(A-H,O-Z)                                         SAT00070
      COMPLEX*16 Z(3)                                                   SAT00080
      INTEGER ISATN                                                     SAT00090
      DIMENSION SAT(4),VR(3),VL(3),VV(3)                                SAT00100
      COMMON/ONE/R,RJPG,A1,B,CAP,TC,PC,W                                SAT00110
      COMMON/FOR/IDELT,IPIZZ,ISATN                                      SAT00120
      DATA ERROR/1.D-6/,EPS/10./,NIT/3000/                              SAT00130
      P=PC                                                              SAT00140
      A=A1*(1.+CAP*(1.-DSQRT(T/TC)))**2                                 SAT00150
10    AA=A*P/(R*T)**2                                                   SAT00160
      BB=B*P/R/T                                                        SAT00170
      SAT(1)=1.                                                         SAT00180
      SAT(2)=BB-1.                                                      SAT00190
      SAT(3)=AA-3.*BB*BB-2.*BB                                          SAT00200
      SAT(4)=BB**3+BB*BB-AA*BB                                          SAT00210
      CALL ZPOLR(SAT,3,Z,IER)                                           SAT00220
      DO 20 J=1,3                                                       SAT00230
      VR(J)=REAL(Z(J))                                                  SAT00240
      VL(J)=VR(J)                                                       SAT00250
      VV(J)=VR(J)                                                       SAT00260
      IF(VR(J).LE.BB) VL(J)=1.D20                                       SAT00270
      IF(VR(J).LE.BB)VV(J)=-1.D20                                       SAT00280
20    CONTINUE                                                          SAT00290
      IF(T.EQ.TC) GO TO 35                                              SAT00300
      ZL=DMIN1(VL(1),VL(2),VL(3))                                       SAT00310
      ZV=DMAX1(VV(1),VV(2),VV(3))                                       SAT00320
      IF(T.EQ.TC) ZL=ZV                                                 SAT00330
      IF(ISATN.EQ.0) GO TO 9                                            SAT00340
      WRITE(6,2)ZL,ZV,P,(VR(J),J=1,3)                                   SAT00350
2     FORMAT(2D15.5,4F10.5)                                             SAT00360
9     CONTINUE                                                          SAT00370
      CONL=(AA/2.828/BB)*DLOG((ZL+2.414*BB)/(ZL-0.414*BB))              SAT00380
      CONV=(AA/2.828/BB)*DLOG((ZV+2.414*BB)/(ZV-0.414*BB))              SAT00390
      FUGL=DEXP(ZL-1.-DLOG(ZL-BB)-CONL)                                 SAT00400
      FUGV=DEXP(ZV-1.-DLOG(ZV-BB)-CONV)                                 SAT00410
      IF(DABS((FUGL-FUGV)/FUGL).LE.ERROR) GO TO 40                      SAT00420
      IF((FUGV-FUGL).LT.0.D0) GO TO 30                                  SAT00430
      P=P-EPS*P*DABS(FUGV-FUGL)                                         SAT00440
      I=I+1                                                             SAT00450
      GO TO 10                                                          SAT00460
30    P=P+EPS*P*DABS(FUGL-FUGV)                                         SAT00470
      I=I+1                                                             SAT00480
      GO TO 10                                                          SAT00490
35    IF(VR(1).EQ.VR(2)) ZL=VR(1)                                       SAT00500
      IF(VR(1).EQ.VR(3)) ZL=VR(1)                                       SAT00510
      IF(VR(2).EQ.VR(3)) ZL=VR(2)                                       SAT00520
      ZV=ZL                                                             SAT00530
40    CONTINUE                                                          SAT00540
      VLSAT=R*T*ZL/P                                                    SAT00550

      VVSAT=R*T*ZV/P                                                    SAT00560
      GO TO 100                                                         SAT00570
80    WRITE(6,1020) NIT,T                                               SAT00580
1020  FORMAT(I10,'   ITERATIONS EXCEEDED IN  SATN AT TEMP:  ',F10.5)    SAT00590
100   CONTINUE                                                          SAT00600
      RETURN                                                            SAT00610
      END                                                               SAT00620
```

```
FILE: ROOT1     FORTRAN  A                    CONVERSATIONAL MONITOR SYSTEM

      FUNCTION ROOT1(T,P)                                                  R0000010
C                                                                          R0000020
C  GIVEN A T (KELVIN) AND P (BARS), ROOT  GIVES                            R0000030
C  THE VOLUME (CC/MOL) IN THE SINGLE PHASE REGION                          R0000040
C  FROM THE PENG-ROBINSON EQ. OF STATE                                     R0000050
C                                                                          R0000060
      IMPLICIT REAL*8 (A-H,O-Z)                                            R0000070
      COMMON/ONE/R,RJPG,A1,B,CAP,TC,PC,W                                   R0000080
      COMPLEX*16 Z(3)                                                      R0000090
      DIMENSION ZR(3),ZI(3),PENG(4)                                        R0000100
      A=A1*(1.+CAP*(1.-DSQRT(T/TC)))**2                                    R0000110
      AA=A*P/R/R/T/T                                                       R0000120
      BB=B*P/R/T                                                           R0000130
      PENG(1)=1.D0                                                         R0000140
      PENG(2)=BB-1.                                                        R0000150
      PENG(3)=AA-3.*BB*BB-2.*BB                                            R0000160
      PENG(4)=BB*BB*BB+BB*BB-AA*BB                                         R0000170
      CALL ZPOLR(PENG,3,Z,IER)                                             R0000180
      DO 10 J=1,3                                                          R0000190
      ZR(J)=REAL(Z(J))                                                     R0000200
      ZI(J)=AIMAG(Z(J))                                                    R0000210
      IF(ZI(J).NE.0.D0) ZR(J)=-1.D25                                       R0000220
      IF(ZR(J).LE.BB) ZR(J)=-1.D25                                         R0000230
10    CONTINUE                                                             R0000240
      ZL=DMAX1(ZR(1),ZR(2),ZR(3))                                          R0000250
      ROOT1=R*T*ZL/P                                                       R0000260
      RETURN                                                               R0000270
      END                                                                  R0000280
```

```
FILE: PIZZA     OUTPUT   A                    CONVERSATIONAL MONITOR SYSTEM

TC= 304.21000  PC=  73.82500  W=   0.22500  VINF=    0.10000D+05
T1= 313.00000  P1= 100.00000
CPA,B,C,D =     0.47280D+01    0.17540D-01   -0.13380D-04    0.40970D-08
DT=    1.00000      IMAX=   100      EPS=     0.10000D+01
ALIMIT=     0.10000D-02     NN =  5
 THE LIQUID SPINOIDAL CURVE WILL BE APPROACHED

 THE ISENTROPIC PATH IS AS FOLLOWS:

TEMPERATURE,KELVIN          PRESSURE,BARS          VOLUME,CC/MOL

      310.155                   91.607                 78.850
      307.379                   83.865                 80.179
      304.678                   76.733                 81.509
      302.020                   70.092                 82.838
      299.484                   64.085                 84.167
```

Appendix III

Solution of the Heat Transfer Problem with Duhamel's Superposition Method

The problem statement is:

$$\frac{\partial\theta}{\partial\xi} = \frac{\partial^2\theta}{\partial\eta^2} \qquad \begin{aligned} \xi &= 0: \quad \theta = 0 \\ \eta &= 0: \quad \theta = 0 \\ \eta &= 1: \quad \theta = -B\xi \end{aligned}$$

Let $\Psi(\xi,\eta)$ be the solution for a unit disturbance:

$$\frac{\partial\Psi}{\partial\xi} = \frac{\partial^2\Psi}{\partial\eta^2} \qquad \begin{aligned} \xi &= 0: \quad \Psi = 0 \\ \eta &= 0: \quad \Psi = 0 \\ \eta &= 1: \quad \Psi = 1 \end{aligned}$$

Try a solution of the form $\Psi(\xi,\eta) = F(\eta) + X(\xi)Y(\eta)$.

The solution to the resulting eigenvalue problem gives:

$$\Psi(\xi,\eta) = \eta + 2\sum_{n=1}^{\infty} \frac{(-1)^n}{n\pi} \sin n\pi\eta \; e^{-n^2\pi^2\xi}$$

The disturbance at the boundary is $D(\xi) = -B\xi$. Solution by Duhamel's superposition method gives:

$$\theta(\xi,\eta) = D(0)\Psi(\xi,\eta) + \int_0^{\xi} \Psi(s,\eta)\,\frac{dD(s)}{ds}\,ds$$

Plugging into this expression:

$$\theta(\xi,\eta) = -B\left[\eta\xi + 2\sum_{n=1}^{\infty} \frac{(-1)^n}{(n\pi)^3} \sin n\pi\eta \; (1 - e^{-n^2\pi^2\xi})\right]$$

Upon differentiation, this yields:

$$\frac{\partial\theta}{\partial\eta} = -B\left[\xi + 2\sum_{n=1}^{\infty}\frac{(-1)^n}{(n\pi)^2}\cos n\pi\eta\,(1 - e^{-n^2\pi^2\xi})\right]$$

Appendix IV

Calculation of the Volume Fraction of Liquid in the Container

The volume of liquid in the filling lines is less than 1% of the container volume, so this will be neglected. It will be assumed that vapor-liquid equilibrium exists.

Define $\underline{V}_{g,L}$ = volume of gas,liquid in the container

$m_{g,L}$ = mass of gas,liquid in the container

m_T = total mass in the container

$\underline{V}_T$ = total volume of the container, which is 7.00 liters or 0.247 ft^3

So, $\underline{V}_g + \underline{V}_L = \underline{V}_T$ and $m_g + m_L = m_T$

For a given pressure, tables of data will give the densities of gas and liquid phases on the saturation curve, ρ_g and ρ_L. These give:

$$\rho_g \underline{V}_g + \rho_L \underline{V}_L = m_T$$

Algebra gives:

$$\frac{\underline{V}_L}{\underline{V}_T} = \frac{(m_T/\underline{V}_T) - \rho_g}{\rho_L - \rho_g} = \text{liquid volume fraction}$$

Since m_T is measured, $\underline{V}_L/\underline{V}_T$ can be determined.

Appendix V

The Flow of an Ideal Gas Through a Sharp-Edged Orifice

From the dimensions of the orifice (burst disc) used in this study, the flow will be critical unless the pressure falls below two bars. So for critical flow through a sharp-edged orifice (Perry and Chilton 1973):

$$W_{max} = -\frac{dN}{dt} = \frac{CAP}{M}\left[\frac{\gamma MK}{RT}\right]^{1/2} \qquad (V\text{-}1)$$

where W_{max} = the maximum flow rate

N = moles of gas in the container

t = time

C = discharge coefficient

A = orifice's cross-sectional area

P = pressure in the container

M = molecular weight of the gas

γ = C_p/C_v, assumed constant

R = gas constant

$K = \left(\frac{2}{\gamma+1}\right)^{\frac{\gamma+1}{\gamma-1}}$

It is assumed that the gas occupies a fixed volume, V, in the container and that it expands adiabatically (i.e., isentropically). For the adiabatic expansion of an ideal gas:

$$T = T_0 \, (P/P_0)^{1-1/\gamma} \qquad (V\text{-}2)$$

where the subscript "0" indicates initial values. Plugging this into the ideal gas equation of state gives:

$$N = \frac{PV}{RT} = \frac{P_0 V}{R T_0}\left(\frac{P}{P_0}\right)^{1/\gamma}$$

Differentiate this with respect to time and use (V-1):

$$-\frac{dN}{dt} = -\frac{V}{RT_0\gamma}\left(\frac{P}{P_0}\right)^{\frac{1}{\gamma}-1}\frac{dP}{dt} = \frac{CAP}{M}\left[\frac{\gamma MK}{RT}\right]^{1/2}$$

Use (V-2) and let $X = P/P_0$ to get :

$$-\frac{dX}{dt} = \frac{CA}{V}\left(\frac{RT_0\gamma^3 K}{M}\right)^{1/2} X^{\frac{3}{2}-\frac{1}{2\gamma}}$$

The solution to this is:

$$\left(\frac{P}{P_0}\right)^{\frac{1-\gamma}{2\gamma}} = 1 - \frac{CA}{V}\left(\frac{RT_0\gamma^3 K}{M}\right)^{1/2}\left(\frac{1-\gamma}{2\gamma}\right) t$$

Appendix VI

Experimental Data

Data for the following saturated experiments are presented.

Expt Number	P_o Initial Pressure, psig(bar)	Liquid Volume Fraction
1	900 (63.1)	0.988
2	" "	0.753
3-WC*	" "	0.902
4	800 (56.2)	0.998
5	" "	0.730
6-WC	" "	0.690
7	650 (45.8)	0.975
8	" "	0.840
9	" "	0.724

Data for the following supercritical experiments are presented.

Expt Number	P_o Initial Pressure, psig(bar)	Specific Volume cm^3/mole
10	1300 (90.7)	59.02
11	1075 (75.2)	133.36
12	" "	98.58
13-WC	1100 (76.9)	81.93

* with wall cooling

P/P_0 for the indicated experiments

time, ms	Experiment Number 1	2	3	4	5	6	7	8	9	10	11	12	13
0	1.000	1.000	1.000	1.000	1.000	1.000	1.000	1.000	1.000	1.000	1.000	1.000	1.000
1	0.923	0.934	0.934	0.902	0.951	0.939	0.759	0.901	0.940	0.947	0.972	0.972	0.946
2	0.913	0.902	0.902	0.877	0.926	0.877	0.699	0.842	0.880	0.878	0.945	0.945	0.928
3	0.902	0.891	0.869	0.865	0.902	0.853	0.639	0.809	0.850	0.848	0.926	0.936	0.901
4	0.902	0.869	0.858	0.853	0.892	0.828	0.594	0.809	0.789	0.802	0.917	0.926	0.883
5	0.891	0.858	0.847	0.840	0.912	0.816	0.579	0.851	0.759	0.779	0.908	0.917	0.865
6	0.880	-	0.825	0.828	0.951	0.804	0.549	0.892	0.729	0.757	0.890	0.908	0.856
7	0.878	0.847	0.814	0.823	0.975	0.791	0.534	0.922	0.699	0.749	0.871	0.899	0.847
8	0.876	0.841	0.803	0.818	0.968	0.779	0.519	0.962	0.669	0.744	0.862	0.890	0.839
9	0.875	0.834	0.792	0.812	0.966	0.767	0.504	0.989	0.639	0.739	0.853	0.871	0.830
10	0.873	0.828	0.781	0.807	0.961	0.755	0.498	0.997	0.609	0.733	0.835	0.862	0.824
11	0.871	0.822	0.770	0.802	0.958	0.742	0.493	0.962	0.579	0.728	0.825	0.853	0.818
12	0.869	0.816	0.759	0.797	0.956	0.742	0.487	0.944	0.564	0.723	0.816	0.844	0.812
13	0.867	0.809	0.750	0.792	0.951	0.730	0.481	0.922	0.549	0.718	0.808	-	0.806
14	0.865	0.803	0.742	0.786	0.946	0.718	0.476	0.907	0.549	0.712	0.801	-	0.800
15	0.864	-	0.733	0.781	0.946	0.705	0.470	0.895	0.549	0.707	0.793	-	0.794
16	0.862		0.724	0.776	-	0.698	0.465	0.884	0.549	0.702	0.785	-	-
17	0.860	-	0.715	0.771	-	0.693	0.459	0.878	-	0.697	0.778	-	-
18	0.858	-	0.707	0.765	-	0.693	0.453	0.877	-	0.691	0.770	-	-
19	0.856	-	0.698	0.760	-	0.693	0.448	0.874	-	0.686	0.762	-	-
20	0.854	-	0.689	0.755	-	0.693	0.442	-	-	0.681	0.754	-	-
spinoidal curve	0.627	0.627	0.627	0.248	0.248	0.248	< 0	< 0	< 0	0.135	0.952	0.822	0.598

Appendix VII
Calculation of an Overall Heat Transfer Coefficient for Runs 5 and 8

For each run, assume:

(1) The liquid expands isentropically until a minimum in the pressure trace is achieved. Boiling starts at this point.

(2) The pressure increases are due to boiling on the vessel's walls.

(3) The vapor volume in the vessel is constant.

(4) Neglect the venting of the vapor during the pressure-increase stage.

(5) CO_2 vapor is an ideal gas.

(6) Temperature does not change appreciably as boiling occurs.

These assumptions will lead to the smallest estimate for the heat transfer coefficient.

For Run 5: The pressure starts at P_o=56.2 bar, reaches a minimum at 0.89 P_o after 4 ms, and reaches a maximum at 0.975 P_o in 3 ms after the minimum.

The temperature driving force, ΔT, is obtained from Figure 4.

$$\Delta T \approx 292 - 291 = 1 \text{ K}$$

The pressure increase rate, $\Delta P/\Delta t$ = 1.59 bar/ms.

The volume of the vapor phase, V = (1-0.73) (7 lit) = 1.89 lit.

The number of moles of CO_2 one must add to this volume to get the observed pressure increase is:

$$\Delta n = \frac{V \ \Delta P}{R \ T_{average}} = 0.38 \text{ mole}$$

From which is obtained : $\Delta n/\Delta t$ = 0.13 mole/ms.

The total heat addition rate, Q, needed to get this boiling rate is:

$$Q = \frac{\Delta n}{\Delta t} \Delta H^V = U A \Delta T$$

where ΔH^V = heat of vaporization. Assume that the value at saturation is a good approximation

= 7190 J/mol at 291 K, from IUPAC (Angus et al., 1973)

U = overall heat transfer coefficient

A = the heat transfer area

= $2\pi(6")(19") = 716\ in^2 = 0.462\ m^2$

Solving for U gives a value of 2×10^2 J/sm^{2}K (3.5×10^5 BTU/hr ft^2 F).

Similarly for Run 8: The pressure starts at P_o=45.8 bar, reaches a minimum at 0.80 P_o after 3.5 ms, and reaches a maximum at P_o in 6.5 ms after the minimum. The pressurization is linear between the minimum and P=0.99 P_o, so this region will be considered.

$$\Delta T \approx 283.5 - 282.5 = 1\ K$$

$$V = (1-0.84)7 = 1.12\ lit$$

$$\Delta n = \frac{(1.12\ lit)(8.7\ b)}{(0.08314)(283\ K)} = 0.41\ mole$$

$$\frac{\Delta n}{\Delta t} = 0.41/5.5 = 0.075\ mol/ms$$

$$\Delta H^V = 8700\ J/mol\ K\ at\ 283K\ (IUPAC)$$

These give $U = 1.4 \times 10^2$ J/sm^{2}K = 2.5×10^5 BTU/hr ft^2 F.

From Perry and Chilton (1973), typical values for heat exchangers are U = 10 to 10^3 BTU/ hr ft^2 F.

Appendix VIII
A Possible Experimental Set-Up
For the Study of Depressurization Explosions

Figure VIII-1 shows a hemispherical container with a cooling jacket and top-closing mechanisms. It is instrumented with pressure transducers and thermocouples. During filling and other preparatory procedures, the flat top is held down by hydraulic piston B, which is mounted on a support that is held in place by hydraulic piston A. While piston B pushes down, springs are attached to the top and stretched so that they pull up on the top.

To depressurize the system, pistons A and B are activated simultaneously: while piston B releases pressure on the top, pistonA pulls piston B out of the top's way. The springs and the internal pressure of the container will blow off the top.

Of course, it will be necessary to have three or more of these spring-piston assemblies on the container at regular intervals to ensure that the top will be secure under the high pressures within the container. To maintain an airtight seal, some sort of O-ring or gasket is needed between the top and the container. The springs may be unnecessary if the top can be fabricated with lightweight materials, so that the internal pressure is sufficient to remove the top. However, the top must be kept from falling back to re-cover the container, so some mechanism (e.g., strong pistons) is needed to prevent this.

As an added precaution, it may be desired to coat the inner surface of the container with Teflon, and to use the wall-cooling procedure. But, if the proposed spring-piston apparatus succeeds in obtaining extremely rapid depressurizations, then these additional concerns may not be of great significance.

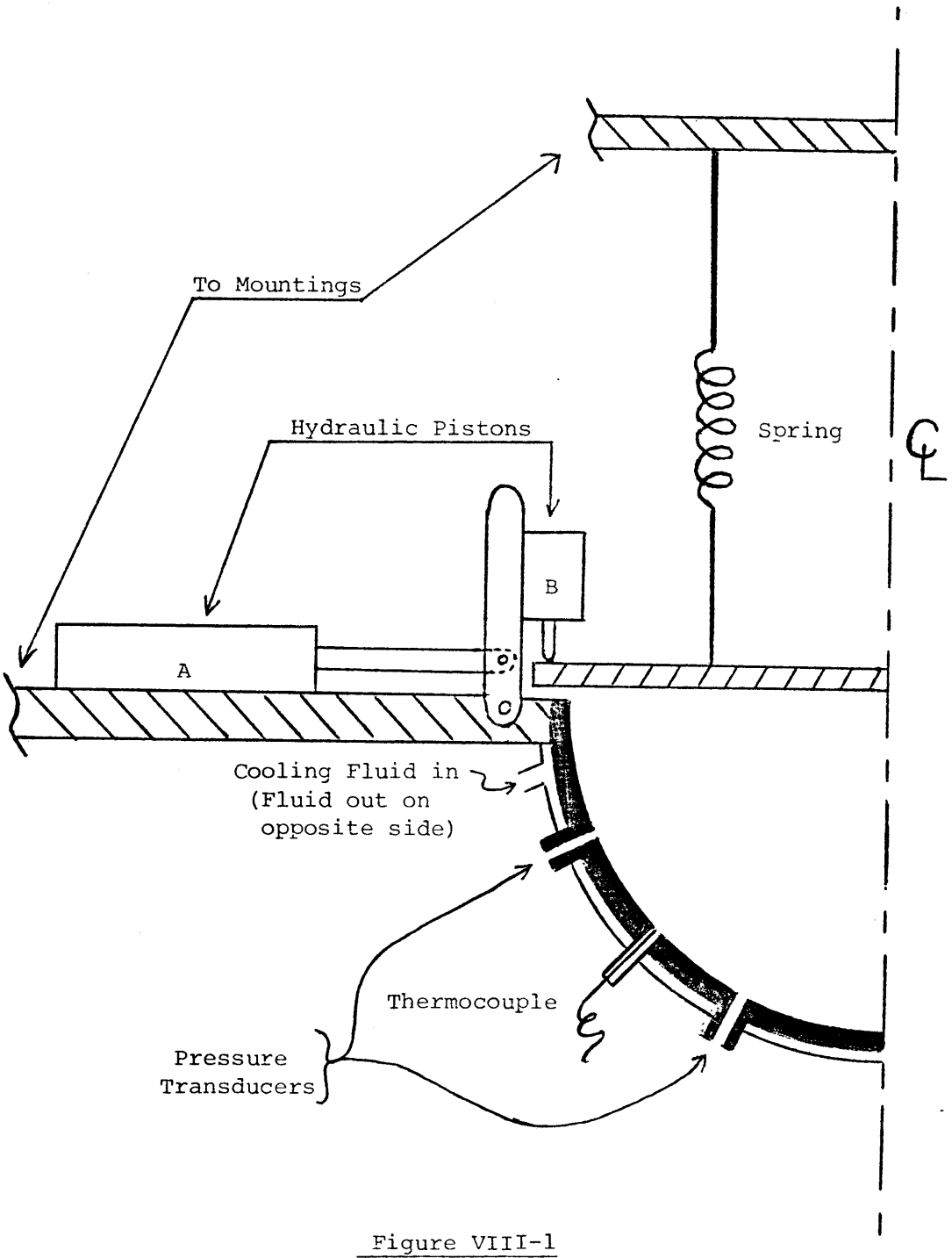

Figure VIII-1

A Possible Experimental Set-Up